Acknowledgments

We thank Dr. Derek LeRoith (The Mount Sinai School of Medicine, NY, USA) and Dr. Hisanori Kato (University of Tokyo) for giving us NIH-3T3 cells over-expressing insulin receptor or IGF-I receptor, and Dr. Toshiaki Ohkuma, Dr. Mitsuhiro Kitajima and Dr. Osamu Fukushi (Fujisawa Pharmaceutical Co., currently Astellas Pharma. Inc., Tokyo, Japan) for the donation of IGF-I. We acknowledge the helpful discussion with Dr. Susan Hall (University of North Carolina at Chapel Hill, NC, USA) and Dr. Asako Takenaka (Meiji University, Kanagawa, Japan). This work was partially supported by Grants-in-Aid from the Japan Society for the Promotion of Science ((A)(2) #16208028, and (A) #22248030), and Program for Promotion of Basic and Applied Researches for Innovations in Bio-oriented Industry to S-IT.

Appendix A. Supplementary data

Supplementary data associated with this article can be found, in the online version, at http://dx.doi.org/10.1016/j.bbrc.2012.05.093.

References

[1] C.M. Taniguchi, B. Emanuelli, C.R. Kahn, Critical nodes in signalling pathways: insights into insulin action, Nat. Rev. Mol. Cell Biol. 7 (2006) 85–96.
[2] J.I. Jones, D.R. Clemmons, Insulin-like growth factors and their binding proteins: biological actions, Endocr. Rev. 16 (1995) 3–34.
[3] Y. Kido, D.J. Burks, D. Withers, J.C. Bruning, C.R. Kahn, M.F. White, D. Accili, Tissue-specific insulin resistance in mice with mutations in the insulin receptor, IRS-1, and IRS-2, J. Clin. Invest. 105 (2000) 199–205.
[4] I. Shimomura, M. Matsuda, R.E. Hammer, Y. Bashmakov, M.S. Brown, J.L. Goldstein, Decreased IRS-2 and increased SREBP-1c lead to mixed insulin resistance and sensitivity in livers of lipodystrophic and ob/ob mice, Mol. Cell 6 (2000) 77–86.
[5] N.J. Kerouz, D. Horsch, S. Pons, C.R. Kahn, Differential regulation of insulin receptor substrates-1 and -2 (IRS-1 and IRS-2) and phosphatidylinositol 3-kinase isoforms in liver and muscle of the obese diabetic (ob/ob) mouse, J. Clin. Invest. 100 (1997) 3164–3172.
[6] C.M. Rondinone, L.M. Wang, P. Lonnroth, C. Wesslau, J.H. Pierce, U. Smith, Insulin receptor substrate (IRS) 1 is reduced and IRS-2 is the main docking protein for phosphatidylinositol 3-kinase in adipocytes from subjects with non-insulin-dependent diabetes mellitus, Proc. Natl. Acad. Sci. U S A 94 (1997) 4171–4175.
[7] L. Rui, M. Yuan, D. Frantz, S. Shoelson, M.F. White, SOCS-1 and SOCS-3 block insulin signaling by ubiquitin-mediated degradation of IRS1 and IRS2, J. Biol. Chem. 277 (2002) 42394–42398.
[8] X. Xu, A. Sarikas, D.C. Dias-Santagata, G. Dolios, P.J. Lafontant, S.C. Tsai, W. Zhu, H. Nakajima, H.O. Nakajima, L.J. Field, R. Wang, Z.Q. Pan, The CUL7 E3 ubiquitin ligase targets insulin receptor substrate 1 for ubiquitin-dependent degradation, Mol. Cell 30 (2008) 403–414.
[9] R. Nakao, K. Hirasaka, J. Goto, K. Ishidoh, C. Yamada, A. Ohno, Y. Okumura, I. Nonaka, K. Yasutomo, K.M. Baldwin, E. Kominami, A. Higashibata, K. Nagano, K. Tanaka, N. Yasui, E.M. Mills, S. Takeda, T. Nikawa, Ubiquitin ligase Cbl-b is a negative regulator for insulin-like growth factor 1 signaling during muscle atrophy caused by unloading, Mol. Cell. Biol. 29 (2009) 4798–4811.
[10] J. Shi, L. Luo, J. Eash, C. Ibebunjo, D.J. Glass, The SCF-Fbxo40 complex induces IRS1 ubiquitination in skeletal muscle, limiting IGF1 signaling, Dev. Cell 21 (2011) pp. 835–847.
[11] L. Rui, T.L. Fisher, J. Thomas, M.F. White, Regulation of insulin/insulin-like growth factor-1 signaling by proteasome-mediated degradation of insulin receptor substrate-2, J. Biol. Chem. 276 (2001) 40362–40367.
[12] T. Haruta, T. Uno, J. Kawahara, A. Takano, K. Egawa, P.M. Sharma, J.M. Olefsky, M. Kobayashi, A rapamycin-sensitive pathway down-regulates insulin signaling via phosphorylation and proteasomal degradation of insulin receptor substrate-1, Mol. Endocrinol. 14 (2000) 783–794.
[13] T. Fukushima, T. Arai, M. Ariga-Nedachi, H. Okajima, Y. Ooi, Y. Iijima, M. Sone, Y. Cho, Y. Ando, K. Kasahara, A. Ozoe, H. Yoshihara, K. Chida, S. Okada, J.J. Kopchick, T. Asano, F. Hakuno, S. Takahashi, Insulin receptor substrates form high-molecular-mass complexes that modulate their availability to insulin/insulin-like growth factor-I receptor tyrosine kinases, Biochem. Biophys. Res. Commun. 404 (2011) 767–773.
[14] T. Kabuta, F. Hakuno, T. Asano, S. Takahashi, Insulin receptor substrate-3 functions as transcriptional activator in the nucleus, J. Biol. Chem. 277 (2002) 6846–6851.
[15] T. Fukushima, T. Nedachi, H. Akizawa, M. Akahori, F. Hakuno, S. Takahashi, Distinct modes of activation of phosphatidylinositol 3-kinase in response to cyclic adenosine 3′,5′-monophosphate or insulin-like growth factor I play different roles in regulation of cyclin D1 and p27Kip1 in FRTL-5 cells, Endocrinology 149 (2008) 3729–3742.
[16] T. Natsume, Y. Yamauchi, H. Nakayama, T. Shinkawa, M. Yanagida, N. Takahashi, T. Isobe, A direct nanoflow liquid chromatography–tandem mass spectrometry system for interaction proteomics, Anal. Chem. 74 (2002) 4725–4733.
[17] F. Hakuno, S. Kurihara, R.T. Watson, J.E. Pessin, S. Takahashi, 53BP2S, interacting with insulin receptor substrates, modulates insulin signaling, J. Biol. Chem. 282 (2007) 37747–37758.
[18] T. Fukushima, H. Okajima, D. Yamanaka, M. Ariga, S. Nagata, A. Ito, M. Yoshida, T. Asano, K. Chida, F. Hakuno, S. Takahashi, HSP90 interacting with IRS-2 is involved in cAMP-dependent potentiation of IGF-I signals in FRTL-5 cells, Mol. Cell. Endocrinol. 344 (2011) 81–89.
[19] M. Li, D. Chen, A. Shiloh, J. Luo, A.Y. Nikolaev, J. Qin, W. Gu, Deubiquitination of p53 by HAUSP is an important pathway for p53 stabilization, Nature 416 (2002) 648–653.
[20] I. Briaud, L.M. Dickson, M.K. Lingohr, J.F. McCuaig, J.C. Lawrence, C.J. Rhodes, Insulin receptor substrate-2 proteasomal degradation mediated by a mammalian target of rapamycin (mTOR)-induced negative feedback down-regulates protein kinase B-mediated signaling pathway in beta-cells, J. Biol. Chem. 280 (2005) 2282–2293.
[21] L.S. Harrington, G.M. Findlay, R.F. Lamb, Restraining PI3K: mTOR signalling goes back to the membrane, Trends Biochem. Sci. 30 (2005) 35–42.
[22] M.E. Sowa, E.J. Bennett, S.P. Gygi, J.W. Harper, Defining the human deubiquitinating enzyme interaction landscape, Cell 138 (2009) 389–403.
[23] W. Li, M.H. Bengtson, A. Ulbrich, A. Matsuda, V.A. Reddy, A. Orth, S.K. Chanda, S. Batalov, C.A. Joazeiro, Genome-wide and functional annotation of human E3 ubiquitin ligases identifies MULAN, a mitochondrial E3 that regulates the organelle's dynamics and signaling, PLoS ONE 3 (2008) e1487.
[24] B. Nicholson, K.G. Suresh Kumar, The multifaceted roles of USP7: new therapeutic opportunities, Cell Biochem. Biophys. 60 (2011) 61–68.
[25] M. Li, C.L. Brooks, N. Kon, W. Gu, A dynamic role of HAUSP in the p53-Mdm2 pathway, Mol. Cell 13 (2004) 879–886.
[26] M. Hu, L. Gu, M. Li, P.D. Jeffrey, W. Gu, Y. Shi, Structural basis of competitive recognition of p53 and MDM2 by HAUSP/USP7: implications for the regulation of the p53-MDM2 pathway, PLoS Biol. 4 (2006) e27.
[27] M. Hu, P. Li, M. Li, W. Li, T. Yao, J.W. Wu, W. Gu, R.E. Cohen, Y. Shi, Crystal structure of a UBP-family deubiquitinating enzyme in isolation and in complex with ubiquitin aldehyde, Cell 111 (2002) 1041–1054.
[28] E. Meulmeester, Y. Pereg, Y. Shiloh, A.G. Jochemsen, ATM-mediated phosphorylations inhibit Mdmx/Mdm2 stabilization by HAUSP in favor of p53 activation, Cell Cycle 4 (2005) 1166–1170.
[29] F. Sarkari, A. La Delfa, C.H. Arrowsmith, L. Frappier, Y. Sheng, V. Saridakis, Further insight into substrate recognition by USP7: structural and biochemical analysis of the HdmX and Hdm2 interactions with USP7, J. Mol. Biol. 402 (2010) 825–837.
[30] A. Takano, I. Usui, T. Haruta, J. Kawahara, T. Uno, M. Iwata, M. Kobayashi, Mammalian target of rapamycin pathway regulates insulin signaling via subcellular redistribution of insulin receptor substrate 1 and integrates nutritional signals and metabolic signals of insulin, Mol. Cell. Biol. 21 (2001) 5050–5062.
[31] Y. Toyoshima, R. Tokita, Y. Ohne, F. Hakuno, T. Noguchi, S. Minami, H. Kato, S.-I. Takahashi, Dietary protein deprivation upregulates insulin signaling and inhibits gluconeogenesis in rat liver, J. Mol. Endocrinol. 45 (2010) 329–340.

Published OnlineFirst April 11, 2012; DOI: 10.1158/1541-7786.MCR-11-0462

Molecular Cancer Research

Signaling and Regulation

SAP155-Mediated Splicing of FUSE-Binding Protein-Interacting Repressor Serves as a Molecular Switch for *c-myc* Gene Expression

Kazuyuki Matsushita[1], Toshiko Kajiwara[1], Mai Tamura[1], Mamoru Satoh[1], Nobuko Tanaka[1], Takeshi Tomonaga[3], Hisahiro Matsubara[2], Hideaki Shimada[4], Rei Yoshimoto[6], Akihiro Ito[6], Shuji Kubo[7], Tohru Natsume[5], David Levens[8], Minoru Yoshida[6], and Fumio Nomura[1]

Abstract

The Far UpStream Element (FUSE)-binding protein-interacting repressor (FIR), a *c-myc* transcriptional suppressor, is alternatively spliced removing the transcriptional repression domain within exon 2 (FIRΔexon2) in colorectal cancers. SAP155 is a subunit of the essential splicing factor 3b (SF3b) subcomplex in the spliceosome. This study aims to study the significance of the FIR–SAP155 interaction for the coordination of *c-myc* transcription, pre-mRNA splicing, and c-Myc protein modification, as well as to interrogate FIRΔexon2 for other functions relating to altered FIR pre-mRNA splicing. Knockdown of SAP155 or FIR was used to investigate their reciprocal influence on each other and on *c-myc* transcription, pre-mRNA splicing, and protein expression. Pull down from HeLa cell nuclear extracts revealed the association of FIR, FIRΔexon2, and SF3b subunits. FIR and FIRΔexon2 were coimmunoprecipitated with SAP155. FIR and FIRΔexon2 adenovirus vector (Ad–FIR and Ad–FIRΔexon2, respectively) were prepared to test for their influence on *c-myc* expression. FIR, SAP155, SAP130, and *c-myc* were coordinately upregulated in human colorectal cancer. These results reveal that SAP155 and FIR/FIRΔexon2 form a complex and are mutually upregulating. Ad–FIRΔexon2 antagonized Ad–FIR transcriptional repression of *c-myc* in HeLa cells. Because FIRΔexon2 still carries RRM1 and RRM2 and binding activity to FUSE, it is able to displace repression competent FIR from FUSE in electrophoretic mobility shift assays, thus thwarting FIR-mediated transcriptional repression by FUSE. Thus aberrant FIRΔexon2 production in turn sustained c-Myc expression. In conclusion, altered FIR and *c-myc* pre-mRNA splicing, in addition to c-Myc expression by augmented FIR/FIRΔexon2–SAP155 complex, potentially contribute to colorectal cancer development. *Mol Cancer Res; 10(6); 787–99. ©2012 AACR.*

Introduction

c-Myc plays a critical role in cell proliferation and tumorigenesis. The *c-myc* proto-oncogene is activated in various tumors, and its ectopic expression generally induces transformation. The expression of c-Myc is tightly regulated in all stages of macromolecular biosynthesis, but how its regulation is coordinated between transcription, pre-mRNA splicing, and c-Myc protein modification remains largely unexplored. The Far UpStream Element (FUSE) is a sequence required for the proper transcriptional regulation of the human *c-myc* gene (1). The FUSE is located 1.5 kb upstream of the *c-myc* promoter P1 and recognized by the FUSE-binding protein (FBP); FBP is a transcription factor that stimulates *c-myc* expression through FUSE (2–4). Yeast 2-hybrid analysis revealed that FBP binds to a protein with transcriptional inhibitory activity termed the FBP-interacting repressor (FIR); by suppressing the TFIIH/p89/XPB helicase, FIR represses *c-myc* transcription (5). Cells from XPB and XPD patients are defective in FIR repression, indicating that mutations in TFIIH impair *c-myc* transcriptional regulation by FIR, which contributes to tumor development (6). In addition, FIRΔexon2, an exon 2 lacking splice variant of FIR devoid of *c-myc* repression activity, is frequently found in human primary colorectal cancers but not in the corresponding noncancerous epithelium, indicating that a dominant, repression-defective FIR could be generated by altered pre-mRNA splicing in cancers (7). Thus, FIRΔexon2

Authors' Affiliations: [1]Department of Molecular Diagnosis (F8), [2]Department of Frontier Surgery (M9), Chiba University Graduate School of Medicine, Chiba City, Chiba; [3]Proteome Research Center, National Institute of Biomedical Innovation, Ibaraki City, Osaka; [4]Department of Gastroenterological Surgery, Toho University Omori Medical Center; [5]Biomedicinal Information Research Center, National Institute of Advanced Industrial Science and Technology, Tokyo, Japan; [6]Chemical Genetics Laboratory, RIKEN Advanced Science Institute, Wako, Saitama, Japan; [7]Department of Genetics, Hyogo College of Medicine, Nishinomiya, Hyogo; and [8]Laboratory of Pathology, National Cancer Institute, Bethesda, Maryland

Note: Supplementary data for this article are available at Molecular Cancer Research Online (http://mcr.aacrjournals.org/).

K. Matsushita and T. Kajiwara contributed equally to this study.

Corresponding Author: Kazuyuki Matsushita, Department of Molecular Diagnosis (F8), Graduate School of Medicine, Chiba University, 1-8-1 Inohana, Chuo-ku, Chiba 260-8670, Japan. Phone: 81-43-226-2167; Fax: 81-43-226-2169; E-mail: kmatsu@faculty.chiba-u.jp

doi: 10.1158/1541-7786.MCR-11-0462

Published OnlineFirst April 11, 2012; DOI: 10.1158/1541-7786.MCR-11-0462

expression has the potential to promote tumor development by disabling authentic *c-myc* repression of FIR; thereby, high levels of c-Myc will sustain growth and often promote apoptosis by increasing the cell division rate, with associated genomic instability and checkpoint-driven apoptosis as consequences.

Splicing factor 3b (SF3b) is a subcomplex of the U2 small nuclear ribonucleoprotein (snRNP) in the spliceosome. SF3b consists of SAP130, SAP145, SAP155, and p14 subunits in nearly equimolar stoichiometry quantities (8). The p14 subunit, cross-linked to the branch point adenosine of pre-mRNA introns within the spliceosome, interacts stably with SAP155, and thus, SF3b is required for intron recognition (9). PUF60, a splicing variant of FIR, is a splicing factor–associated protein (8, 10). However, how FIR directly or indirectly interacts with U2 snRNPs is not yet known. Recently, SAP155 was found to directly bind to PUF60 (11, 12), but this was not determined in the case of FIR. In addition, 2 natural chemical derivatives, spliceostatin A (SSA; ref. 13) and pladienolide (14), inhibit SF3b and thereby induce an antitumor effect. These results imply that SF3b normally promotes tumors.

In this study, the SAP155-mediated regulation of FIR/FIRΔexon2 expression was investigated along with its pre-mRNA splicing in *c-myc* gene expression. We examined SF3b expression in excised human colorectal cancer tissues, effects of SAP155 knockdown or SSA treatment on FIR pre-mRNA splicing, and total protein expression of FIRs in terms of c-Myc repression. We found that SAP155 is required for FIR expression and vice versa, and that SAP155 regulates alternative splicing of FIR. Both FIR and FIRΔexon2 were pulled down with SAP155. Importantly, FIRΔexon2 could markedly enhance c-Myc expression, whereas FIR suppresses c-Myc expression. Thus, sustained FIR/FIRΔexon2–SAP155 interaction affects the well-established functions of FIR and SAP155, and hence, interferes with transcription and alternative splicing of *c-myc* gene, respectively. In addition, the reason why FIR, FIRΔexon2, and SAP155 are activated in colorectal cancers is also discussed.

Materials and Methods

Excised human tumor samples

Tissues from 34 cases of primary colorectal cancer were surgically excised at Chiba University Hospital. The tumor samples were obtained from tumor epithelium immediately after surgical excision, and corresponding nontumor epithelial samples were taken 5 to 10 cm away from the tumor. Two pathologists microscopically confirmed all tissue samples as adenocarcinomas. All excised tissues were immediately placed in liquid nitrogen and stored at −80°C until analysis. Written informed consent was obtained from each patient before surgery.

Cell culture

HeLa, HCT116, and 293T cell lines were purchased from American Type Culture Collection (ATCC) and stored in the liquid nitrogen before use. Cells were grown at 37°C in 5% CO_2 in Iscove's Modified Dulbecco's Medium (IMDM) supplemented with 10% FBS (Invitrogen) and 1% penicillin–streptomycin (Invitrogen).

Protein extraction from tissue samples and immunoblotting

Proteins from whole-cell extracts were dissolved in a sample buffer as described previously (7). The amount of protein in the supernatant was measured by a protein assay (Bio-Rad). The proteins were separated by electrophoresis on polyacrylamide gels of suitable concentration and transferred to a polyvinylidene fluoride membrane (Millipore) using a tank transfer apparatus (Bio-Rad). The membrane was blocked with 5% skim milk in PBS for 1 hour.

Western blot and antibodies

Protein extracts were separated by electrophoresis on a 7.5% to 15% Perfect NT Gel (DRC). Proteins were then transferred to polyvinylidene fluoride membranes (Millipore) using a tank transfer apparatus (Bio-Rad). The membranes were blocked with 0.5% skim milk in PBS. The primary mouse monoclonal antibody against FIR C-terminus (6B4) was prepared by Dr Nozaki (15). Briefly, the synthetic peptide was used as immunization antigen (Supplementary Fig. S2B; ref. 16). Anti-FIR rabbit polyclonal antibodies were prepared or purchased from Japan BioService. Other primary and secondary antibodies are listed in Supplementary Table S1. Antigens on the membrane were detected with enhanced chemiluminescence detection reagents (GE Healthcare, UK Ltd). The intensity of each band was measured by NIH Image.

Plasmids

Full-length FIR cDNA was cloned into a p3xFLAG-CMV-14 vector (Sigma) to introduce a FLAG-tag at the carboxyl terminus, and FIRΔexon2 cDNA was cloned into a pcDNA 3.1 plasmid (Invitrogen). Myc-tag at the carboxyl terminus was prepared by PCR with suitable primers, including restriction enzyme sites (*Bgl*II and *Xba*I; Supplementary Table S2) through FIR- or FIRΔexon2-FLAG-tag vector. Plasmids were prepared by CsCl ultracentrifugation or using the Endofree Plasmid Maxi Kit (Qiagen) and DNA sequences were verified.

Stable transfection

Cells were transfected with plasmids using Lipofectamine 2000 reagents (Gibco BRL). For stable transfection, 5×10^4 cells were transfected with the above FIR-FLAG or pcDNA3.1-FIRΔexon2 plasmids and transferred to 10-cm dishes 48 hours after transfection. The complete medium contained 400 μg/mL geneticin in addition to IMDM, 10% FBS, and 1% penicillin–streptomycin. The complete medium with geneticin was replaced every 4 days until geneticin-resistant colonies appeared. At least 30 clones were screened by immunoblotting and immunostaining with anti-FLAG and anti-FIR antibodies (6B4) to find FIR-FLAG expressing clones for FIR-FLAG stably expressing

Published OnlineFirst April 11, 2012; DOI: 10.1158/1541-7786.MCR-11-0462

cells, or with anti-c-Myc antibody to examine c-Myc expression for FIRΔexon2 stably expressing cells.

Extraction of nuclear protein and immunoprecipitation (pull-down assay)

Cells (~1 × 10^8) were resuspended in 5 mL cold buffer [50 mmol/L phosphate (pH-8.0), 20 mmol/L NaCl, 1 mmol/L DTT, 0.1% NP-40, protease inhibitor cocktail (Roche Diagnostics)] and left on ice for 15 minutes. The cells were then homogenized in a Dounce homogenizer or vigorously vortexed twice for 15 seconds before being centrifuged for 5 minutes at 100 ×*g*. After the pellet was washed twice with the same cold buffer, it was solubilized in lysis buffer [50 mmol/L phosphate buffer (pH 8.0), 150 mmol/L NaCl, 1 mmol/L DTT, 0.1% NP-40, and protease inhibitor cocktail] and then centrifuged for 1 hour at 20,000 ×*g*. The supernatant nuclear proteins were then used in a Western blot.

For immunoprecipitation by anti-FLAG antibody–conjugated beads, the nuclear fraction (NF) was reacted with magnetic Magnosphere MS300/carboxyl beads (Como Bio) precoated with anti-mouse IgG to reduce nonspecific protein binding and then reacted with anti-FLAG antibody for 1 hour at 4°C. After immunoprecipitation, the IgG and anti-FLAG antibody–conjugated beads were washed 5 times with 50 mmol/L phosphate buffer and the bound proteins were eluted with extraction buffer [40 mmol/L Tris-HCl (pH 6.8), 1% SDS, 1 mmol/L DTT] for 1 hour at 60°C. The immunoprecipitates were then analyzed by gel-based liquid chromatography-mass spectrometry (GeLC-MS) and protein identification (17). For immunoprecipitation by anti-SAP155 antibody–conjugated beads, Dynabeads ProteinG (Invitrogen) was prepared by same procedures as anti-FLAG antibody. After immunoprecipitation with NF, anti-SAP155 antibody–conjugated beads were washed 5 times with 100 mmol/L Glycine (WAKO Pure Chemical Industries Ltd.; pH 2.0) for 10 minutes at 4°C.

FIR binding protein identification

Exhaustive screening of FIR binding proteins was carried out using 2 independent methods. One was GeLC-MS (18–20) via Flag-conjugated bead pull down with LC-MS. Digested peptides were injected into a 0.3 × 5-mm L-trap column and a 0.1 × 150-mm L-column2 (Chemicals Evaluation and Research Institute, Saitama, Japan) attached to a NanoSpace high-performance liquid chromatography (HPLC) pump (Shiseido Fine Chemicals) and Magic 2002 splitter (AMR). The flow rate of the mobile phase was 500 nL/min. The solvent composition of the mobile phase was programmed to change in 60-minute cycles with varying mixing ratios of solvent A (2% v/v CH_3CN and 0.1% v/v HCOOH) to solvent B (90% v/v CH_3CN and 0.1% v/v HCOOH): 5% to 45.5% B 35 minute, 45.5% to 90% B 4 minute, 90% B 0.5 minute, 90%–5% B 1 minute, 5% B 20 minute. Purified peptides were introduced from HPLC to LTQ XL (Thermo Scientific), an ion-trap mass spectrometer, via an attached PicoTip (New Objective). The Mascot search engine (Matrixscience) was used to identify proteins from the mass and tandem mass spectra of the peptides. Peptide mass data were matched by searching the Human International Protein Index database [IPI, July. 2009, 80412 entries, European Bioinformatics Institute (Cambridge, UK)] using the MASCOT engine. Database search parameters were peptide mass tolerance 1.2 Da; fragment tolerance, 0.6 Da; enzyme set to trypsin, allowing up to one missed cleavage; variable modifications, methionine oxidation. Identification data (MASCOT dat file) were organized by Scaffold 3.0.2 software (Proteome Software, Inc.). The minimum criteria for protein identification were protein and peptide thresholds set to 95.0% (Scaffold's probability threshold filter) and number of unique peptides set to 2. The methods for the direct nanoflow liquid chromatography-tandem mass spectrometry (LC/MS-MS) system with FIR-FLAG transiently transfected 293T nuclear extracts have been described previously (21).

Immunocytochemistry

The FIR-FLAG stably expressing HeLa cells were grown on coverslips overnight and then subjected to immunocytochemistry as described previously (7). The primary mouse monoclonal anti-FLAG (Santa Cruz Biotechnology) and primary polyclonal antibodies against SAP155 were diluted 1:500 and 1:200, respectively, in the blocking buffer. The coverslips were incubated at room temperature for 1 hour. After washing with PBS, the secondary antibodies Alexa Fluor 488–conjugated goat anti-rabbit or 594-conjugated goat anti-mouse IgG secondary antibody (Molecular Probes) was applied at a dilution of 1:1,000. DNA was counterstained with 4′, 6-diamidino-2-phenylindole (DAPI) III (Vysis, Abbott Park) and cells were observed under an immunofluorescence microscope (Leica QFISH; Leica Microsystems). Other primary and secondary antibodies used in this study are listed in Supplementary Table S1.

siRNA against FIR or SAP155

FIR and SAP155 siRNA duplexes were purchased from Sigma Aldrich. The target sequences for FIR siRNA and SAP155 siRNA oligonucleotides are listed (Supplementary Table S2). Transient transfection of siRNA was carried out using Lipofectamine 2000 (Invitrogen) according to the manufacturer's instructions. The transfected cells were cultured for 72 hours at 37°C in a CO_2 incubator.

Reverse transcriptase PCR and quantitative real-time PCR

Total RNA was extracted from HeLa cells using the RNeasy Mini Kit (Qiagen). cDNA was synthesized from total RNA by the first strand cDNA Synthesis Kit for reverse transcriptase PCR (RT-PCR; Roche). Using the cDNA as a template, FIR cDNA was amplified with suitable primers by RT-PCR (Supplementary Table S2). Glyceraldehyde-3-phosphate dehydrogenase cDNA was amplified and used as the control. The PCR product was loaded on a 2.5% agarose gel (Promega), purified with the Gel Extraction Kit (Qiagen) and cloned using the pGEM-T Easy vector system (Promega) for DNA sequencing.

Published OnlineFirst April 11, 2012; DOI: 10.1158/1541-7786.MCR-11-0462

Quantitative real-time PCR (qRT-PCR) for *c-myc* or FIR cDNA was done using the LightCycler (Roche) in 20 μL of reaction mixture consisting of a master mixture (LightCycler FastStart DNA Master SYBR Green I) that contained FastStart Taq DNA polymerase, dNTPs, and buffer (LightCycler DNA Master hybridization probes; Roche), 3.0 mmol/L $MgCl_2$, 0.5 μmol/L each of sense and antisense primers, and 1 μL of template cDNA in a LightCycler capillary. LightCycler software version 3.3 (Roche) was used for the analysis of real-time RT-PCR. Primer and probe sets for β-actin were purchased from Roche Diagnostics. Primers for RT-PCR and qRT-PCR, siRNAs were purchased and used simultaneously in accordance with the manufacturer's instructions (Nihon Gene Research Laboratories Inc.; Supplementary Table S2). Locations of primers and probes for real-time PCR in this study are indicated for FIR, FIRΔexon2, Δ3, and Δ4 cDNAs (Supplementary Fig. S2C).

Spliceostatin A, SF3b (SAP155) inhibitor, and adenovirus vectors

SSA was prepared as previously (13). The FIR and FIRΔexon2 adenovirus vector was also prepared (Supplementary Fig. S1). Briefly, recombinant adenoviral vectors expressing full-length human FIR proteins were constructed by homologous recombination in *Escherichia coli* using the AdEasy XL system (Stratagene). The *Hind*III-*Pme*I fragment of pcDNA3.1-FIR (/FIRΔexon2) or the *Hind*III-*Eco*RV fragment of pcDNA3.1-CMV-LacZ or pcDNA3.1-CMV-GFP was cloned into the *Hind*III–*Eco*RV site of pShuttle-CMV, generating pShuttle-CMV-FIR (otherwise FIRΔexon2), pShuttle-CMV-LacZ or pShuttle-CMV-GFP (as controls). The resultant shuttle vectors were linearized with *Pme*I digestion and subsequently cotransfected into *E. coli* BJ5183-AD-1. The recombinants were linearized with *Pac*I digestion and transfected into the E1 transcomplementing 293 cell line to generate Ad-FIR (FIRΔexon2) and Ad-LacZ. The viruses were propagated in the adenovirus packaging 293 cell line (ATCC) and purified by double CsCl density gradient centrifugation followed by dialysis in 10 mmol/L Tris buffer (pH 8.0) with 10% glycerol. The virus titer was determined by conventional limiting dilution of 293 cells, that is, a plaque-forming assay was carried out with 293 cells ($TCID_{50}$ method). The viruses were aliquoted and stored at −80°C until use. The recombinant adenovirus vectors were used to examine the effect to c-Myc expression.

FIR or FIRΔexon2 protein preparation

To reduce the dimerization, the C-terminal (95 amino acids)-truncated FIR (447 a.a.) or FIRΔexon2 (418 a.a), including FIR RRM1+RRM2 (Supplementary Fig. S2B and C), was cloned into *Nde*I/*Xho*I site of pET21b vector (Novagen; Merck chemicals) to introduce His-Tag at C-terminal and then was transfected to BL21-CodonPlus (DE3)-RIPL competent cells (Stratagene). Culture was carried out in TB medium (Invitrogen) in the presence of 100 μg/mL ampicillin and 34 μg/mL chloramphenicol. Expression was introduced with 0.5 mmol/L IPTG and then culture was continued at 30°C for 4 hours. Cells were harvested by centrifugation and disrupted by sonication in PBS. The supernatants from centrifugation were applied to HisTrap HP (GE Healthcare) and eluted by imidazole linear gradient. The eluted proteins were dialyzed to 50 mmol/L Tris/HCl, pH8.0, then applied HiTrap Q HP column (GE Healthcare). FIR or FIRΔexon2 was eluted NaCl linear gradient (0.2 to 1.0 mol/L). The eluted proteins were concentrated and loaded to HiLoad16/60 Superdex75pg gel filtration column (GE Healthcare), then eluted by 50 mmol/L Tris/HCl, 150 mmol/L NaCl, 10% glycerol, pH8.0 at 0.5 mL/min.

FUSE ssDNA oligonucleotides

All ssDNA oligonucleotides and 5′- or 3′-biotinylated ssDNA oligonucleotides pools were chemically synthesized (Nihon Gene Research Laboratories).

Electrophoresis mobility shift assay (gel shift assay)

FIR or FIRDexon2 protein binding assay with FUSE antisense ssDNA oligonucleotides was carried out by LightShift Chemiluminescent electrophoresis mobility shift assay (EMSA) Kit. EBNA-1 protein and EBNA-1 binding DNA sequence was employed as positive control (Thermo Scientific) according to company's instruction.

Statistical analysis

Comparison of SAP130, SAP145, SAP155, and FIR expression between cancer tissues and noncancer epithelium was evaluated using the Student *t* test. Correlation between FIR and SAP155 expression was evaluated using the Pearson product–moment correlation coefficients.

Results

Relationship among FIR, FIRΔexon2, and SF3b subunits expression in colorectal cancer tissues

PUF60 is an SF3b-associated protein (8, 12), and FIR is a splicing variant of PUF60 that lacks exon 5. Total FIR is increased in colorectal cancers (7). Recently, SSA (13) and pladienolide (14) have been reported to inhibit SF3b and induce a strong antitumor effect, implying that SF3b normally promotes tumors. Therefore, we examined SF3b expression in surgically excised human colorectal cancers (Fig. 1A and B). Total FIR and SF3b subunit levels were increased in colorectal cancers tissues compared with their corresponding nontumor epithelia (Fig. 1C). Furthermore, the levels of total FIR, SAP155, and SAP130 were positively correlated (Fig. 1C). However, the level of SAP145, another component with nearly equimolar subunit stoichiometry with the other essential subunits of SF3b, was paradoxically lower in cancer relative to SAP155 and SAP130 expression (Fig. 1A and B). *c-myc*, SAP155, SAP130, FIR, FIRΔexon2, and the ratio of FIRΔexon2/FIR were all increased at the mRNA level in colon cancer tissues (T) compared with corresponding noncancer epithelium (N; Fig. 1D). These results suggested that total FIRs, SAP155, or SAP130 tightly correlate with each other and may cooperate during tumor formation and progression, perhaps to elevate c-Myc.

Published OnlineFirst April 11, 2012; DOI: 10.1158/1541-7786.MCR-11-0462

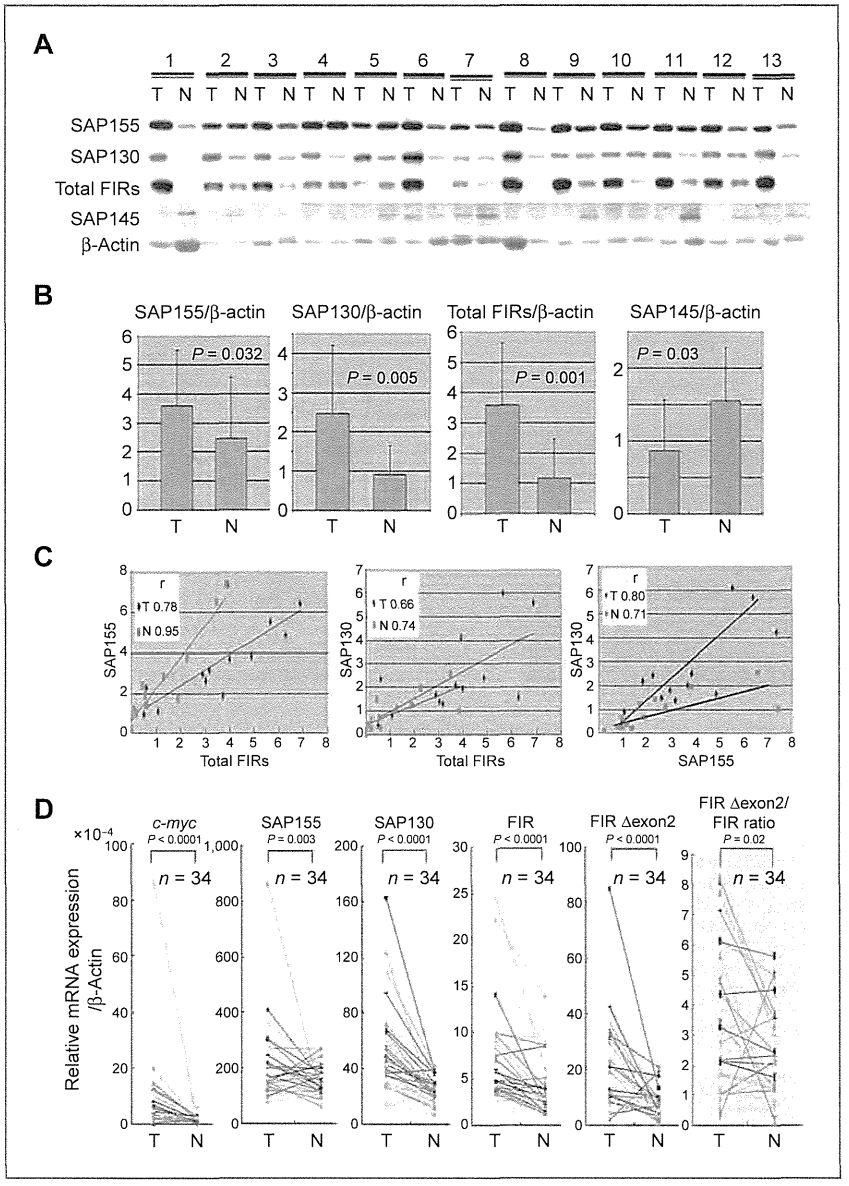

Figure 1. SAP155 and SAP130, SF3b subunits were activated in a positive correlation with FIR in colon cancer tissues. A, total protein lysates were prepared from 30 matched tumor samples (T) and adjacent nontumor epithelial tissue (N). FIR, SAP155, and SAP130 were activated, whereas SAP145 was downregulated in colorectal cancer tissues. β-Actin was used as an internal control. B, the intensity of each band was measured by NIH image, and the relative mean of SAP155, SAP130, FIR, and SAP145 protein levels between (T) and (N) with β-actin were calculated. Histogram indicating that SAP155, SAP130, and FIR expression levels in (T) were significantly higher than those in (N; $P = 0.032$, 0.005, and 0.001 from a t test, respectively). Inversely, SAP145 expression was significantly higher in (N) than in (T; $P = 0.03$ from a t test). Note, the P value of the SAP155 and SAP145 comparison is borderline acceptable. C, FIR–SAP155, FIR–SAP130, and SAP155–SAP130 expression in each colorectal cancer tissue sample was correlated between (T) and (N). The Pearson product–moment correlation coefficients (r) were 0.78 (T) and 0.95 (N) for FIR–SAP155, 0.66 (T) and 0.74 (N) for FIR–SAP130, and 0.80 (T) and 0.71 (N) for SAP155–SAP130. D, *c-myc*, FIR, FIRΔexon2, SAP155, and SAP130 mRNAs were all significantly activated in colon cancer tissues compared with the corresponding nontumor epithelium. *c-myc* and FIRΔexon2 mRNAs were definitely overexpressed, and the ratio of FIRΔexon2/FIR mRNA was increased.

FIR and FIRΔexon2 were coimmunoprecipitated and colocalized with SAP155, indicating FIR, FIRΔexon2, and SAP155 potentially forms a complex

By immunoprecipitation, SAP155 associated with FIR (Fig. 2A, top). Subcellular localization analysis of FIR and SAP155 showed that these 2 proteins colocalized in the nucleoplasm (Fig. 2A, bottom). To show whether SAP155, FIR, and FIRΔexon2 directly interact with each other, FLAG-tag or Myc-tag recombinant proteins were stably or transiently expressed in HeLa cells. Then reciprocal pull-down assays among those proteins were carried out (at least 3 replicates each). Association between FIR-SAP155 (Fig. 2B, top and bottom panels, arrowheads), FIRΔexon2 interacted strongly with SAP155 regardless of which partner was tagged (Fig. 2B, top and bottom, arrows), FIR also interacted more strongly with FIRΔexon2 (Fig. 2C, left, arrow), than with itself (Fig. 2C, left, arrowhead) and FIRΔexon2 also was strongly self-interacting (Fig. 2C, right, arrow). SAP155 was pull down with FIR- and FIRΔexon2-containing complexes, but SAP130 was not detected (Fig. 2C). Therefore, it is likely that FIR and SF3b are functionally linked. The dynamics and affinities among FIR,

Published OnlineFirst April 11, 2012; DOI: 10.1158/1541-7786.MCR-11-0462

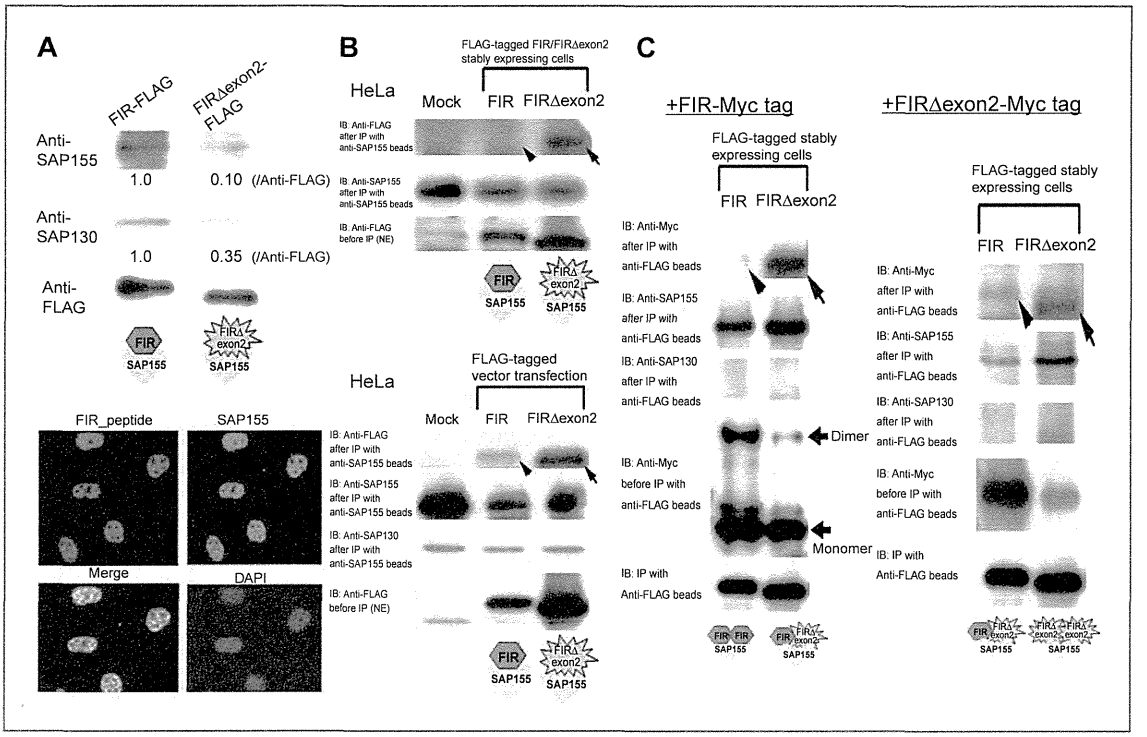

Figure 2. FIR, FIRΔexon2, and SAP155 forms complex. A, proteins associated with anti-FLAG beads in the nuclear extracts of FIR–FLAG- or FIRΔexon2–FLAG stably expressing HeLa cells were analyzed with Western blot using anti-SAP155 or SAP130 antibodies. SAP155 and SAP130 were much less detectable in the FIRΔexon2–FLAG complex, 0.10 and 0.35, compared with the FIR–FLAG complex at 1.0, respectively (top). Immunofluorescent study showed that endogenous total FIRs (red) and SAP155 (green) were colocalized in the nucleoplasm. Both endogenous total FIRs and SAP155 were also colocalized in the nucleus (bottom). B, to examine the interaction between FIR or FIRΔexon2 and SAP155, FIRΔexon2 or FIR was pulled down with anti-SAP155–conjugated beads in nuclear extracted proteins (NE) of FIR/FIRΔexon2-FLAG stably (top) or transiently (bottom) expressing HeLa cells. The eluted proteins were immunoblotted with anti-FLAG antibody to examine the association between FIR/FIRΔexon2 and SAP155 (top). NE of FIR/FIRΔexon2-FLAG transiently expressing HeLa cells were prepared and treated with anti-SAP155–conjugated beads. The eluted proteins were immunoblotted with anti-FLAG antibody to examine the association between FIR/FIRΔexon2 and SAP155 (bottom). C, to examine the interaction between FIR-FIR, FIR-FIRΔexon2, or FIRΔexon2-FIRΔexon2, FIR-FLAG or FIRΔexon2-FLAG was pulled down with anti-FLAG–conjugated beads in NEs of FIR-Myc tag (top) or FIRΔexon2-Myc-tag (bottom) transiently expressing HeLa cells. NEs of FIR/FIRΔexon2-FLAG stably expressing HeLa cells were prepared and either FIR-Myc tag (top) or FIRΔexon2-Myc-tag (bottom) expressing vector was transfected. Then the eluted proteins were immunoblotted with anti-FLAG or anti-Myc antibody to examine the association between FIR-FIR, FIR-FIRΔexon2, or FIRΔexon2-FIRΔexon2, respectively. Note, SAP155 was apparently pulled down with FIR-FIR or FIR-FIRDexon2 complex, but SAP130 was below detection level. IB, immunoblotting.

FIRΔexon2, and SAP155 and their relationship to cancer await further studies.

SAP155 regulates alternative splicing of FIR pre-mRNA and amounts of endogenous total FIR proteins

To gain insight into the physiologic relationship between FIR and SAP155, we first examined the effect of SAP155 knockdown by siRNA on the splicing and expression of FIR. Treatment of HCT116 or HeLa cells with SAP155 siRNA for 48 hours induced an altered splicing pattern of FIR (Fig. 3A, arrows) and a reduction in the total amount of endogenous FIRs. Novel FIR splicing variants, Δ3 (Exons 1, 3, and 6–12) and Δ4 (Exons 1, 6–12), were found (Fig. 3A and B, Supplementary Fig. S2A and C). Analysis using quantitative real-time PCR (qRT-PCR; Fig. 3A, bottom panels) showed that the ratio of Δ3 and Δ4 mRNA relative to FIR mRNA was increased by the SAP155 siRNA treatment in HCT116 and HeLa cells, and the ratio of FIRΔexon2 mRNA relative to FIR mRNA was increased in HeLa cells (Fig. 3A, bottom panels). SSA, an SF3b inhibitor, was used to verify the role of SAP155 in the alternative splicing of FIR mRNA. Although SAP155 expression was not suppressed by SSA, FIR pre-mRNA splicing was affected, just as was seen using SAP155 siRNA (Fig. 3B, arrows). SSA treatment generated the FIR splicing variants Δ3 and Δ4, revealed by DNA sequencing of RT-PCR products (Fig. 3B and Supplementary Fig. S2A and C). These results indicated that pattern of FIR splicing is sensitive to the level or function of SAP155.

So why did the knockdown of SAP155 by siRNAs reduce the amount of endogenous total FIR (Fig. 3A)? Is SAP155 required for endogenous FIR expression? To examine whether FIR and SAP155 interact with each other, we next tested whether FIR knockdown could also reduce SAP155 expression. FIR siRNA treatment reciprocally decreased the

Published OnlineFirst April 11, 2012; DOI: 10.1158/1541-7786.MCR-11-0462

SAP155 protein level, but not the SAP155 mRNA level, in HeLa and HCT116 cells (Fig. 3C). These results indicated that FIR and SAP155 form a complex at the protein level but that FIR does not significantly affect the SAP155 mRNA level. For proper expression, FIR requires SAP155 at the RNA level, but SAP155 requires FIR at the protein level.

SAP155 and SAP130, but not SAP145, were coimunoprecipitated with FIR

The expression of FIR and SF3b subunits SAP155 and SAP130, but not SAP145, significantly correlated in colon cancer (Fig. 1C). FIR seems to have a significantly higher affinity for SAP155 by pull-down assay (Fig. 2B–2D), whereas SF3b consists of SAP130, SAP145, and SAP155 subunits in nearly equimolar stoichiometry amounts (8). To explore this discrepancy, we carried out exhaustive screening of FIR-binding proteins using 2 independent analyses. One was gel-enhanced LC/MS-MS (GeLC/MS-MS) analysis using FLAG-conjugated bead pull down with FIR– or FIRΔexon2–FLAG stably transfected HeLa cell nuclear extracts (refs. 18–20; Supplementary Table S3). The other was a direct nano-LC/MS-MS system with FLAG-conjugated bead pull down with FIR– or FIRΔexon2–FLAG transiently transfected 293T cell nuclear extracts (refs. 21–24; Supplementary Table S4). In both exhaustive screenings in HeLa cells, SAP155 was pulled down with FIR, but none of SAP155, SAP130, or SAP145 coimmunoprecipitated with FIRΔexon2. In 293T cells, SAP155 and SAP130 were pulled down with FIR and FIRΔexon2, respectively (Supplementary Table S5).

SF3b is a highly stable protein complex that remains intact at high ionic strengths (25, 26). If SF3b is highly stable, how does SAP155 encounter FIR and form stable complexes? We hypothesize that SAP155 encounters FIR before forming the SF3b complex. If this is true, the synthesis of authentic SF3b should be hindered because of the imbalance in SAP155, SAP145, and SAP130 proportions, and thus, SF3b dysfunction might occur in cancer cells. In this scenario, the elevated FIR–SAP155 complexes in colorectal cancers modify their predominant activities in nonneoplastic cells, FIR as a *c-myc* transcriptional repressor and SF3b as a splicing factor.

SeV/ΔF/FIR suppressed SSA-activated c-Myc, whereas Ad–FIRΔexon2 activated c-myc transcription and led to c-Myc overexpression

To determine whether the increase in *c-myc* is likely attributable to the reduced FIR activity in cells, the SeV/ΔF/FIR (27) was used in attempt to block the increase in c-Myc that results from treatment with either SAP155 siRNA or SSA. SeV/ΔF/FIR suppressed SSA-induced c-Myc activation (Fig. 4A, compare lane 2 with lane 1) but not basal c-Myc expression (Fig. 4A, compare lanes 4 to 3 and 6 to 5, respectively). These results were consistent with previous reports that FIR suppresses activated, not basal, *c-myc* transcription (5). Ad–FIRΔexon2 activates not only *c-myc* transcription but also c-Myc protein expression in HeLa cells (Fig. 4B). As expected, FIR antagonized the upregulation of MYC by FIRΔexon2 (Fig. 4C). How should we interpret this result? c-Myc mRNA and protein are not in a linear relationship because c-Myc increases the efficiency of translation, including its own mRNA mediated by coding region determinant-binding protein/insulin-like growth factor 2 mRNA binding protein 1 (CRD-BP/IGF2BP-1; refs. 28, 29). Notably, CRD-BP/IGF2BP-1 was coimmunoprecipitated with both FIR and FIRΔexon2 (Supplementary Table S5). These observations suggested that the increase in *c-myc* from either the SAP155 siRNA or SSA treatment is likely due to the reduced FIR or an imbalance between FIR and FIRΔexon2 in HeLa cells. Together, FIRΔexon2-FIR and SAP155 serves as molecular switches for *c-myc* expression.

Reduction of SAP155 elevates c-Myc expression with FIR suppression in HeLa cells

As SAP155 knockdown reduced the expression of FIR, a *c-myc* transcriptional repressor, it is possible that c-Myc expression is regulated, at least partly, by SAP155. Indeed, SAP155 siRNA apparently increased c-Myc but decreased FIR protein expression in HeLa cells (Fig. 5A). Accordingly, c-Myc activation by SAP155 siRNA is likely to be indirect via FIR. SAP155 siRNA also reduced the level of SAP130 (Fig. 5B), suggesting that SAP155, SAP130, and FIR form a complex. Thus, to further examine the relationship between c-Myc protein expression and FIRΔexon2, we measured the ratio of FIRΔexon2/FIR mRNA during SAP155 knockdown (Fig. 5C) or SSA treatment (Fig. 5D). As anticipated, the ratio of FIRΔexon2/FIR mRNA correlated well with c-Myc protein expression in those cells. These findings indicated that the disturbance of FIR pre-mRNA splicing, and thus the ratio of FIRΔexon2/FIR mRNA, had an effect on not only *c-myc* gene transcription, but also on c-Myc protein levels during SAP155 knockdown or SSA treatment.

c-myc gene intron was actively transcripted in colon cancer tissues

These results strongly suggested that FIR has a higher affinity with SF3b, SAP155, and SAP130. Hence, in cancer cells, it is likely that SAP155/FIR or SAP155/130/FIR form alternative complexes to the ordinary SF3b complex, and that this may disturb *c-myc* pre-mRNA splicing. Actually, *c-myc* gene intron 1 sequences were relatively more abundant in cancers in which the expression of the SF3b subunits was disturbed than in adjacent noncancer epithelia (Fig. 6A). Of note, unspliced *c-myc* mRNA was also overproduced in cancers (7). RT-PCR using a variety of primer sets showed that SAP155 siRNA increased total *c-myc* mature mRNA (Fig. 5A), as well as immature *c-myc* intron 1-containing mRNA (Fig. 6B) levels. These results confirmed that total *c-myc* transcription was activated by SAP155 knockdown. In addition, it is possible that SSA severely impairs *c-myc* pre-mRNA splicing (Fig. 6C). FIR siRNA also slightly inhibited *c-myc* pre-mRNA splicing (Fig. 6D). Collectively, disturbed FIR or SAP155 expression at least partly affected both *c-myc* gene transcription and splicing in human colon cancer tissues.

Published OnlineFirst April 11, 2012; DOI: 10.1158/1541-7786.MCR-11-0462

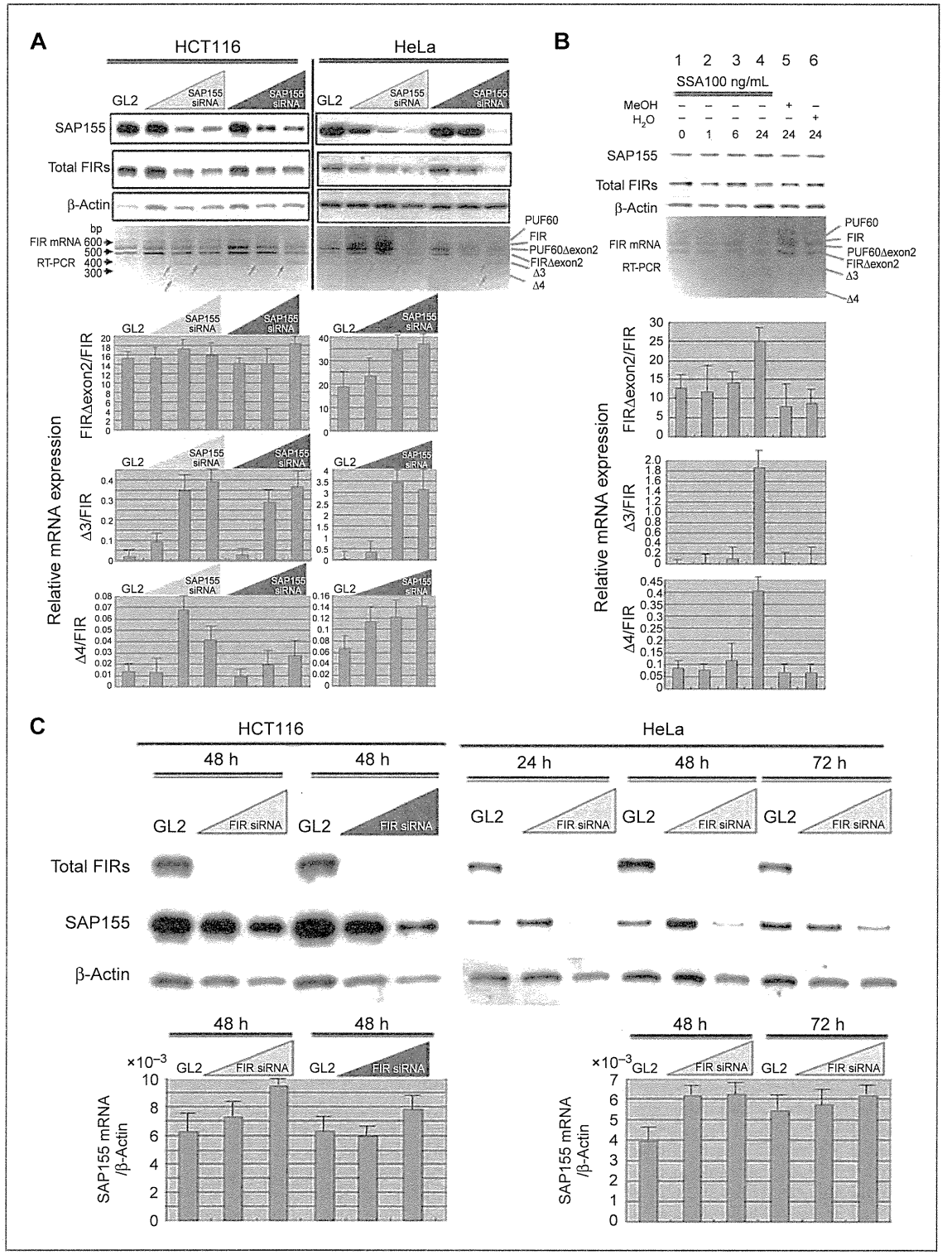

Published OnlineFirst April 11, 2012; DOI: 10.1158/1541-7786.MCR-11-0462

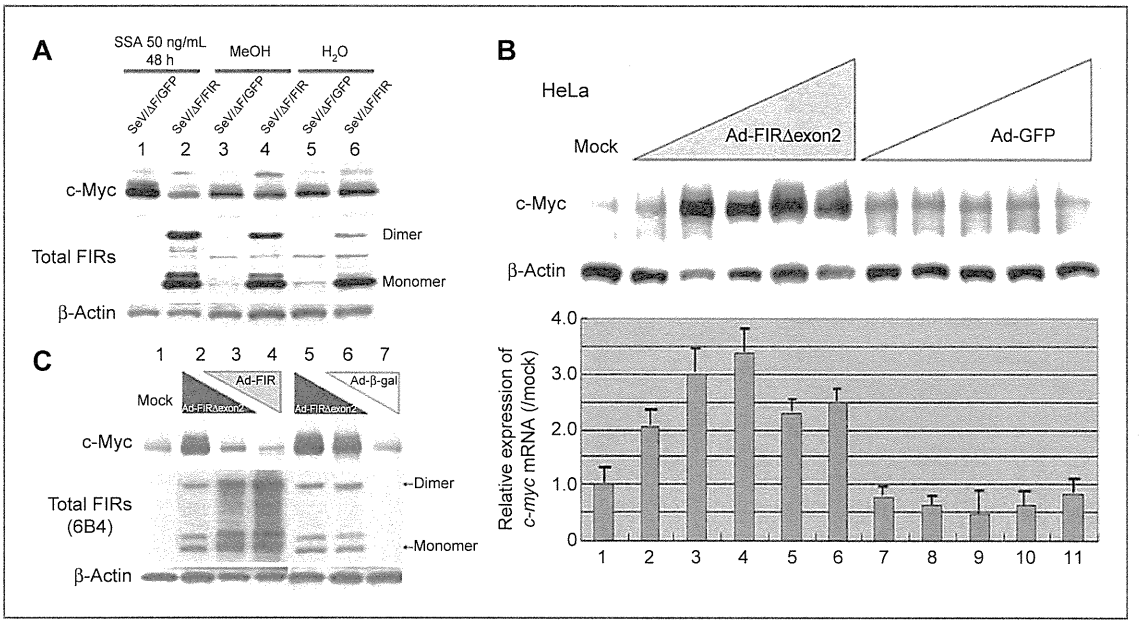

Figure 4. Ad–FIR suppressed SSA-activated c-Myc, whereas Ad–FIRΔexon2 activated *c-myc* transcription and led to c-Myc overexpression. A, c-Myc activation in 50 ng/mL SSA treatment for 48 hours was suppressed by enforced SeV/ΔF/FIR expression (lane 2). The effect of SeV/ΔF/FIR (27) was examined for whether the increase in c-Myc from either the SAP155 siRNA or SSA treatment is impaired by FIR. SeV/ΔF/FIR suppressed SSA-induced c-Myc activation (compare lane 2 with lane 1), but not basal c-Myc expression (compare lanes 4 and 6 with lanes 3 and 5, respectively). B, HeLa cells were treated with Ad–FIRΔexon2 for 48 hours, and whole cell proteins and total RNAs were extracted. Western blot analysis for c-Myc protein expression and qRT-PCR for *c-myc* mRNA were carried out. Ad–FIRΔexon2 activated c-Myc protein and *c-myc* mRNA in HeLa cells. Ad–GFP was used as a control vector. Mock shows that HeLa crude extract proteins are not subject to adenovirus vector treatment. Lanes 2, 7: 0.1 MOI; lanes 3, 8: 0.5 MOI; lanes 4, 9: 1 MOI; lanes 5, 10: 5 MOI; lanes 6, 11: 10 MOI of Ad–FIRΔexon2 or Ad–GFP, respectively. Ad–FIRΔexon2 apparently increased c-Myc more than 20 times over mock expression, whereas Ad–GFP did not affect c-Myc. The increase of *c-myc* mRNA was much less, 2 to 3 times that of c-Myc protein elevation by Ad–FIRΔexon2. C, FIR and Ad–FIRΔexon2 antagonized against c-Myc expression (compare lanes 3 and 6). Lane 1 (Mock): no adenovirus vector; Lane 2: 10 MOI of Ad–FIRΔexon2; Lane 3: 5 MOI of Ad–FIRΔexon2 and 5 MOI of Ad–FIR; Lane 4: 10 MOI of Ad–FIR; Lane 5: 10 MOI of Ad–FIRΔexon2 (same as lane 2); Lane 6: 5 MOI of Ad–FIRΔexon2 and 5 MOI of Ad–β-gal; Lane 7: 10 MOI of Ad–β-gal. Notably, *c-myc* mRNA was not significantly activated by Ad–FIRΔexon2 (data not shown). MOI, multiplicity of infection.

FIRΔexon2ΔC interferes FIRΔC to bind to FUSE

FIRΔC- or FIRΔexon2ΔC-His tag proteins that deleted C-terminal 95 amino acids, containing RRM1 and RRM2, were purified (Fig. 7A). FIRΔexon2ΔC was found to interfere with FIRΔC binding to FUSE via EMSA (Fig. 7B). FIR and FIRΔexon2 form complex (Fig. 2C). These results indicated that formation of FIRΔexon2 competes with FIR for binding to FUSE; probably the protein–protein interaction interferes with DNA recognition by RRM1. A model of summarizing the consequences of FIRΔexon2's interactions with FIR and with SAP155/SAP130 is shown in Fig. 7C. FIR suppresses *c-myc* gene transcription and SAP155 regulates alternative splicing in noncancer cells (Fig. 7C, left), whereas FIRΔexon2 interferes with FIR binding to FUSE, resulting *c-myc* activation with potent SF3b dysfunction in cancer cells (Fig. 7C, right)

Discussion

The results of this study are summarized as follows: (i) FIRΔexon2 interacts with FIR and SAP155 (ii) siRNA

Figure 3. siRNA knockdown of SAP155 reduces FIR levels and vice versa. A, treatment with SAP155 siRNA for 48 hours suppressed FIR protein expression and FIR pre-mRNA splicing in HCT116 and HeLa cells. RT-PCR of full-length FIR cDNAs isolated from HeLa or HCT116 cells was carried out to amplify the aminoterminal regions. Note that novel FIR splicing variants, Δ3 and Δ4, were induced by SAP155 siRNA detected by RT-PCR (bottom, arrows). The expression levels of FIR and FIRΔexon2 mRNAs were quantified by qRT-PCR after SAP155 siRNA treatment for 48 hours in HCT116 and HeLa cells (bottom). The ratios of Δ3 and Δ4 mRNA relative to FIR mRNA were increased by the SAP155 siRNA treatment in HCT116 and HeLa cells, as well as the ratio of FIRΔexon2/FIR mRNA in HeLa cells. There was no significant alteration of the ratio of FIRΔexon2/FIR mRNA expression by SAP155 siRNA in HCT116 cells. B, effects of SSA, an SF3b inhibitor, on endogenous FIR expression and pre-mRNA splicing in HeLa cells were analyzed by qRT-PCR. Total FIRs expression was reduced by treatment with 100 ng/mL SSA for 24 hours. Altered FIR pre-mRNA splicing (lane 4) was detected by qRT-PCR in SSA-treated cells. Novel FIR splicing variants, Δ3 and Δ4, were accumulated by SSA treatment as well as by SAP155 siRNA, as shown in Fig. 1A. The ratios of FIRΔexon2, Δ3, and Δ4 mRNA relative to FIR mRNA were increased by SSA treatment. C, FIR siRNA suppressed SAP155 expression in HeLa and HCT116 cells for 48 hours. The ratio of SAP155/β-actin mRNA was not suppressed by FIR siRNA as determined by qRT-PCR.

Published OnlineFirst April 11, 2012; DOI: 10.1158/1541-7786.MCR-11-0462

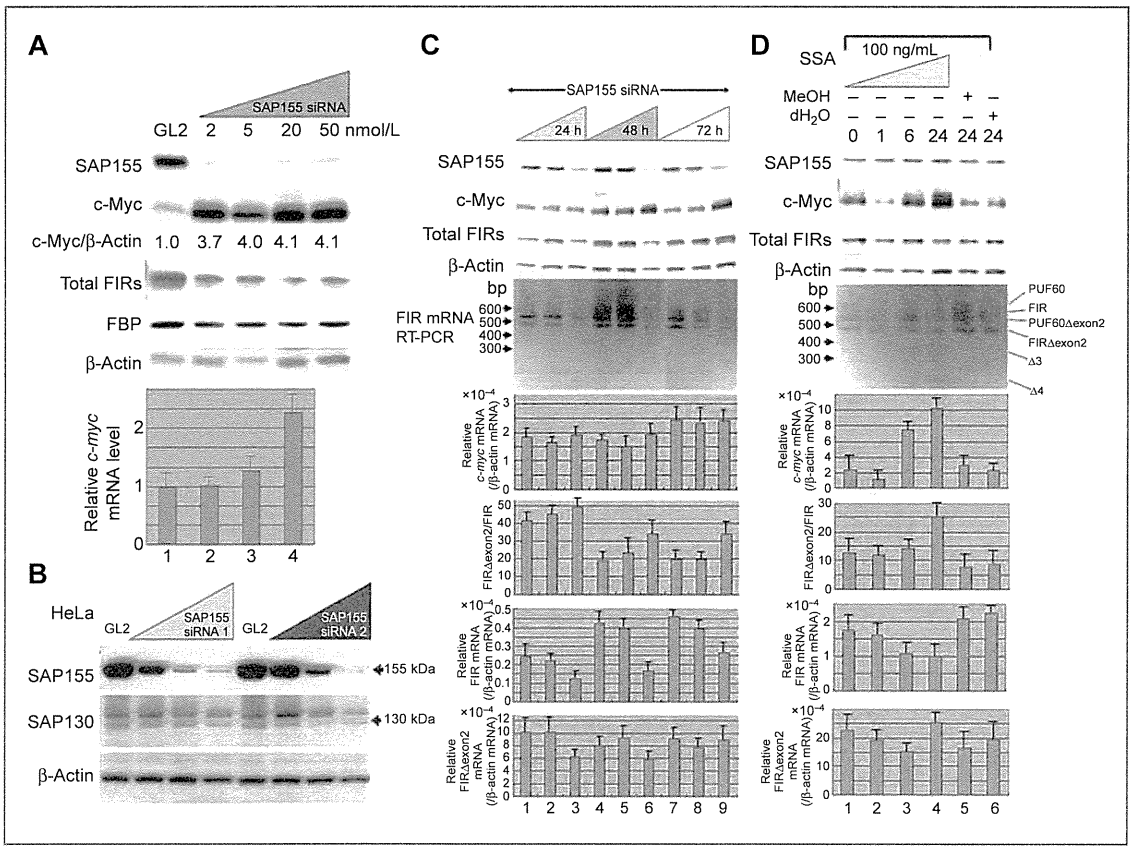

Figure 5. The ratio of FIRΔexon2/FIR mRNA coincided well with c-Myc expression. A, treatment with SAP155 siRNA at the indicated concentrations for 48 hours induced an increase in *c-myc* mRNA, as determined by qRT-PCR, and protein and a decrease in FIR protein expression. FBP expression was unchanged by SAP155 siRNA. Knockdown of SAP155 by siRNA apparently increased c-Myc about 4 times more than mock expression. Notably, the increase of *c-myc* mRNA was, at most, 2 times more than GL2. B, knockdown of SAP155 by siRNA also decreased SAP130 expression in HeLa cells. C, interestingly, c-Myc activation was partly transcriptional because *c-myc* mRNA determined by qRT-PCR was increased along with SAP155 siRNA. The ratio of FIRΔexon2/FIR mRNA determined by qRT-PCR; FIRΔexon2/FIR mRNA coincided well with c-Myc protein expression level. D, SSA (100 ng/mL) was administered in a time-dependent manner to HeLa cells. MeOH: an equal amount of methanol that dissolves SSA was used as a control; H_2O: an equal amount of H_2O that dissolves SSA was used as another control. Interestingly, *c-myc* mRNA and c-Myc protein expression levels correlated well with the ratio of FIRΔexon2/FIR mRNA expression rather than with FIR or FIRΔexon2 mRNA expression alone.

knockdown of FIR reduces SAP155 levels and vice versa; (iii) increased levels of FIRΔexon2 and siRNA knockdown of SAP155 increased c-Myc levels; and (iv) FIRΔexon2 potently interferes with FIR binding to FUSE, yielding ineffective suppression of *c-myc*. In other words, augmented and sustained FIR/FIRΔexon2–SAP155 interaction modifies the functions of FIR and SAP155, thereby interfering with *c-myc* transcription and alternative splicing, respectively. In cancer cells, alternative splicing of FIR or *c-myc* pre-mRNA may also be disturbed (8). FIR/FIRΔexon2–SAP155 complex formation potently disturbs the proportion of SAP155, SAP130, and SAP145 in SF3b, thus altering FIR pre-mRNA and changing the ratio of FIRΔexon2 to FIR mRNA expression. SAP155 siRNA or SSA treatment induces transient c-Myc activation in HeLa cells (Fig. 5A, C, and D). Reduction of FIR increases *c-myc* expression, and overexpression of FIRΔexon2 leads to c-Myc protein activation. Thus, this process forms a novel *bona fide* molecular switch for *c-myc* gene expression.

Why were both FIR and FIRΔexon2 overexpressed in colorectal cancer tissues? Why was SAP155 activated in cancer tissues, although SAP155 siRNA or SSA treatment induced c-Myc. First reason might be that FIR is a c-Myc target. Also, the tight FIR/FIRΔexon2–SAP155 interaction disables established FIR and SAP155 functions disturbing the synthesis of normally spliced FIR mRNA. Second, FIRΔexon2 potently forms a heterodimer with FIR (Fig. 2B–D) and thus FIRΔexon2 interferes with FIR to bind to FUSE (Fig. 7B and C). These results strongly suggest that FIRΔexon2 antagonized FIR in *c-myc* transcriptional suppression and simultaneously interferes with SF3b in splicing during tumor progression. Third, genomic or somatic

Published OnlineFirst April 11, 2012; DOI: 10.1158/1541-7786.MCR-11-0462

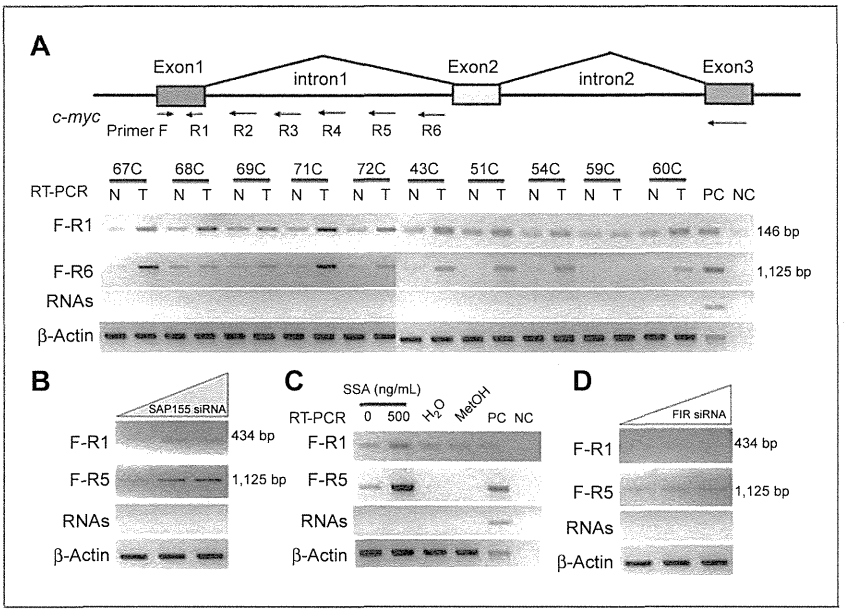

Figure 6. Endogenous *c-myc* gene splicing was altered in colon cancer tissues. Total RNA was extracted from 5 matched, operatively excised human tumor samples (T) and adjacent nontumor epithelial tissue (N). cDNA was synthesized from RNA. *c-myc* intron 1 was examined to determine the extent of transcription by RT-PCR, through changing the reverse primers located in *c-myc* intron 1 (R2–R6). A, primers for detection of transcribed *c-myc* intron 1 are listed in Supplementary Table S2. *c-myc* intron 1 was disturbed and transcribed in (T) but not in (N). PC: positive control (cDNA synthesized by HeLa cell total mRNA); NC: negative control (H_2O). B, treatment with SSA (500 ng/mL) disturbed transcription of *c-myc* intron 1. Transcription of *c-myc* intron 1 was also apparently disturbed by siRNA against SAP155 (C) and FIR (D). RNAs: PCR was carried out with primers F-R1 and F-R6 with 1 μg of extracted total RNA as a template to exclude genomic DNA contamination.

SAP155 is mutated in cancers (30, 31). How would these SAP155 somatic mutations affect to the regulation of c-Myc by FIR and its alternative splicing products? SAP155 somatic mutations observed in cancers accumulated at a specific site, supporting a gain-of-function of SAP155, and perhaps strengthening binding with FIR or FIRΔexon2. The FBP–FIR–FUSE system mediates *c-myc* transcriptional control because the RNA recognition motifs of FIR provide a platform for independent FUSE DNA and FBP protein binding, and this explains the structural basis of the reversibility of the FBP–FIR interaction (32, 33). Does FIRΔexon2 interfere with the dimerization of FIR on nucleic acid binding? What we do know is that the first RNA recognition motif (RRM) of FIR (amino acids 112–187-RRM1, Supplementary Fig. S2C) binds nucleic acids, and thus, it would be helpful to examine whether a conformational change would occur in FIRΔexon2 because FIR has been shown to dimerize upon nucleic acid binding (33).

At least one alternative splicing variant is present in 60% to 95% of all human genes (34). Does the FIR/FIRΔexon2–SAP155 complex affect alternative splicing in addition to FIR or the *c-myc* gene? Although further studies are required to answer this question, the disturbance of alternative splicing by SSA treatment has been found only in limited genes (35). Transcription affects splicing and vice versa, but much remains to be learned about how these processes are coupled (36–38). How does FIRΔexon2 activate *c-myc*? Does FBP–FIR or FIR–SAP155 binding differ among noncancer, transformed, and cancer cells? FBP was identified as a FIR- or FIRΔexon2-binding protein in 293T cells (Supplementary Tables S4 and S5), but it was below the detection levels in HeLa nuclear extracts (Supplementary Tables S3 and S4).

The existence of proteins binding uniquely to FIR or FIRΔexon2, as well as of proteins binding to both (Supplementary Fig. S4A) between FIR and FIRΔexon2 in HeLa cells (Supplementary Table S3) and 293T cells (Supplementary Table S5) suggests that this system can be tuned depending on the cell conditions. IGF2BP-1/CRD-BP, which meditates stabilization of *c-myc* mRNA and in turn transcriptionally regulated by *c-myc* (28, 29), was coimmunoprecipitated with both FIR and FIRΔexon2 (Supplementary Table S5). Accordingly, the balance of *c-myc* transcription, splicing patterns as well as *c-myc* mRNA stability can be adjusted differently in different cells or in tumors because authentic FIR function in *c-myc* transcriptional repression and SAP155 in alternative splicing were simultaneously disturbed by FIR/FIRΔexon2/SAP155 complex formation. Our study proposes that *c-myc* is regulated not only at the transcriptional but also by the efficiency of the splicing of its pre-mRNA. Further studies of agents that modify FIR/FIRΔexon2-SAP155 complex formation and SAP155 inhibitors (39) may provide clues to cancer therapy.

Published OnlineFirst April 11, 2012; DOI: 10.1158/1541-7786.MCR-11-0462

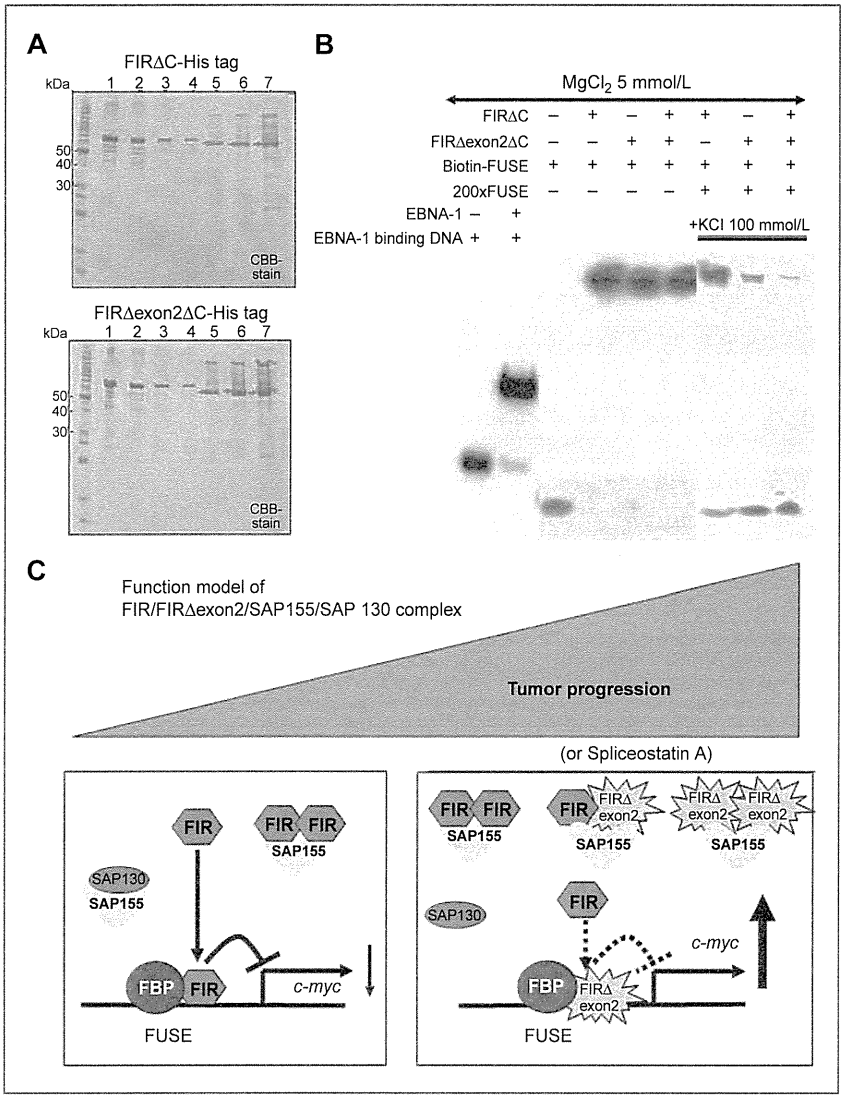

Figure 7. FIRΔexon2 potentially interferes with FIR to bind to FUSE along with tumor progression. A, C-terminal 95 amino acids deleted FIR- or FIRΔexon2-His tag protein, FIRΔC- or FIRΔexon2ΔC-His tag or with FIR-RRM1 and RRM2 (amino acids 103–297, exons 6–9), was prepared, purified, and was analyzed by SDS-PAGE. After affinity purification by HisTrapHP, recovered sample was dialyzed against 50 mmol/L Tris-HCl (pH9.0). Lane 1; 1,000 ng of bovine serum albumin (BSA), lane 2; 500 ng of BSA, lane 3; 250 ng of BSA, lane 4; 125 ng of BSA, lane 5; 2 μL, lane 6; 4 μL, lane 7; 8 μL of purified FIR- (top) or FIRΔexon2-His tag (bottom) proteins. Concentration of FIRΔexon2-His tag proteins was estimated by band intensity using with BSA as a standard. B, EMSA revealed that FIRΔexon2ΔC interferes with FIRΔC to bind to FUSE. C, functional model of FIR/FIRΔexon2/SAP155/SAP130 complex along with tumor progression. FIR suppresses *c-myc* gene transcription and SAP155 engages in alternative splicing in noncancer cells, whereas potential FIR, FIRΔexon2, and SAP155 complex disturbed authentic FIR and SAP155 function simultaneously in cancer cells.

Disclosure of Potential Conflicts of Interest

No potential conflicts of interest were disclosed.

Acknowledgments

The authors thank Dr. Naohito Nozaki at the Department of Biochemistry and Molecular Biology, Kanagawa Dental College, Yokosuka, Kanagawa, for preparation of FIR monoclonal antibodies.

Grant Support

This study was supported in part by grant-in-aid 18591453 for priority areas in cancer research from the Ministry of Education, Science, Sports and Culture of Japan and "Seed Finding Programs" and "Mini-Feasibility Study Project" of JST (Japan Science and Technology) Agency to K. Matsushita, and Grant-in-Aid for Scientific Research (S) from the Japan Society for the Promotion of Science to R. Yashimoto and M. Yoshido.

The costs of publication of this article were defrayed in part by the payment of page charges. This article must therefore be hereby marked *advertisement* in accordance with 18 U.S.C. Section 1734 solely to indicate this fact.

Received September 20, 2011; revised January 24, 2012; accepted March 25, 2012; published OnlineFirst April 11, 2012.

References

1. Avigan MI, Strober B, Levens D. A far upstream element stimulates *c-myc* expression in undifferentiated leukemia cells. J Biol Chem 1990;265:18538–45.
2. Duncan R, Bazar L, Michelotti G, Tomonaga T, Krutzsch H, Avigan M, et al. A sequence-specific, single-strand binding protein activates the far upstream element of *c-myc* and defines a new DNA-binding motif. Genes Dev 1994;8:465–80.
3. Bazar L, Meighen D, Harris V, Duncan R, Levens D, Avigan M. Targeted melting and binding of a DNA regulatory element by a transactivator of *c-myc*. J Biol Chem 1995;270:8241–8.

Published OnlineFirst April 11, 2012; DOI: 10.1158/1541-7786.MCR-11-0462

4. Michelotti GA, Michelotti EF, Pullner A, Duncan RC, Eick D, Levens D. Multiple single-stranded cis elements are associated with activated chromatin of the human *c-myc* gene *in vivo*. Mol Cell Biol 1996;16:2656–69.
5. Liu J, He L, Collins I, Ge H, Libutti D, Li J, et al. The FBP interacting repressor targets TFIIH to inhibit activated transcription. Mol Cell 2000;5:331–41.
6. Liu J, Akoulitchev S, Weber A, Ge H, Chuikov S, Libutti D, et al. Defective interplay of activators and repressors with TFIH in xeroderma pigmentosum. Cell 2001;104:353–63.
7. Matsushita K, Tomonaga T, Shimada H, Shioya A, Higashi M, Matsubara H, et al. An essential role of alternative splicing of *c-myc* suppressor FIR in carcinogenesis. Cancer Res 2006;66:1409–17.
8. Will CL, Urlaub H, Achsel T, Gentzel M, Wilm M, Lührmann R. Characterization of novel SF3b and 17S U2 snRNP proteins, including a human Prp5p homologue and an SF3b DEAD-box protein. EMBO J 2002;21:4978–88.
9. Spadaccini R, Reidt U, Dybkov O, Will C, Frank R, Stier G, et al. Biochemical and NMR analyses of an SF3b155-p14-U2AF-RNA interaction network involved in branch point definition during pre-mRNA splicing. RNA 2006;12:410–2.
10. Hastings ML, Allemand E, Duelli DM, Myers MP, Krainer AR. Control of pre-mRNA splicing by the general splicing factors PUF60 and U2AF (65). PLoS One 2007;2:e538.
11. Mollet I, Barbosa-Morais NL, Andrade J, Carmo-Fonseca M. Diversity of human U2AF splicing factors. FEBS J 2006;273:4807–16.
12. Corsini L, Hothorn M, Stier G, Rybin V, Scheffzek K, Gibson TJ, et al. Dimerization and protein binding specificity of the U2AF homology motif of the splicing factor Puf60. J Biol Chem 2009;284:630–9.
13. Kaida D, Motoyoshi H, Tashiro E, Nojima T, Hagiwara M, Ishigami K, et al. Spliceostatin A targets SF3b and inhibits both splicing and nuclear retention of pre-mRNA. Nat Chem Biol 2007;3:576–83.
14. Kotake Y, Sagane K, Owa T, Mimori-Kiyosue Y, Shimizu H, Uesugi M, et al. Splicing factor SF3b as a target of the antitumor natural product pladienolide. Nat Chem Biol 2007;3:570–5.
15. Kimura K, Nozaki N, Enomoto T, Tanaka M, Kikuchi A. Analysis of M phase-specific phosphorylation of DNA topoisomerase II. J Biol Chem 1996;271:21439–45.
16. Page-McCaw PS, Amonlirdviman K, Sharp PA. PUF60: a novel U2AF65-related splicing activity. RNA 1999;5:1548–60.
17. Kristjansdottir K, Wolfgeher D, Lucius N, Angulo DS, Kron SJ. Phosphoprotein profiling by PA-GeLC-MS/MS. J Proteome Res 2008;7:2812–24.
18. Tomonaga T, Matsushita K, Ishibashi M, Nezu M, Shimada H, Ochiai T, et al. Centromere protein H is up-regulated in primary human colorectal cancer and its overexpression induces aneuploidy. Cancer Res 2005;65:4683–9.
19. Seimiya M, Tomonaga T, Matsushita K, Sunaga M, Oh-Ishi M, Kodera Y, et al. Identification of novel immunohistochemical tumor markers for primary hepatocellular carcinoma; clathrin heavy chain and formiminotransferase cyclodeaminase. Hepatology 2008;48:519–30.
20. Nishimori T, Tomonaga T, Matsushita K, Oh-Ishi M, Kodera Y, Maeda T, et al. Proteomic analysis of primary esophageal squamous cell carcinoma reveals downregulation of a cell adhesion protein, periplakin. Proteomics 2006;6:1011–8.
21. Natsume T, Yamauchi Y, Nakayama H, Shinkawa T, Yanagida M, Takahashi N, et al. A direct nanoflow liquid chromatography-tandem mass spectrometry system for interaction proteomics. Anal Chem 2002;74:4725–33.
22. Mizushima N, Kuma A, Kobayashi Y, Yamamoto A, Matsubae M, Takao T, et al. Mouse Apg16L, a novel WD-repeat protein, targets to the autophagic isolation membrane with the Apg12-Apg5 conjugate. J Cell Sci 2003;116:1679–88.
23. Yanagida M, Hayano T, Yamauchi Y, Shinkawa T, Natsume T, Isobe T, et al. Human fibrillarin forms a sub-complex with splicing factor 2-associated p32, protein arginine methyltransferases, and tubulins alpha 3 and beta 1 that is independent of its association with pre-ribosomal ribonucleoprotein complexes. J Biol Chem 2004;279:1607–14.
24. Komatsu M, Chiba T, Tatsumi K, Iemura S, Tanida I, Okazaki N, et al. A novel protein-conjugating system for Ufm1, a ubiquitin-fold modifier. EMBO J 2004;23:1977–86.
25. Brosi R, Hauri HP, Krämer A. Separation of splicing factor SF3 into two components and purification of SF3a activity. J Biol Chem 1993;268:17640–6.
26. Das BK, Xia L, Palandjian L, Gozani O, Chyung Y, Reed R. Characterization of a protein complex containing spliceosomal proteins SAPs 49, 130, 145, and 155. Mol Cell Biol 1999;19:6796–802.
27. Kitamura A, Matsushita K, Takiguchi Y, Shimada H, Tomonaga T, Matsubara H, et al. Synergistic effect of non-transmissible Sendai virus vector encoding the c-myc suppressor FUSE-binding protein-interacting repressor plus cisplatin in treatment of malignant pleural mesothelioma. Cancer Sci 2011;102:1366–73.
28. Noubissi FK, Nikiforov MA, Colburn N, Spiegelman VS. Transcriptional regulation of CRD-BP by c-myc: implications for c-myc functions. Genes Cancer 2010;10:1074–82.
29. Noubissi FK, Elcheva I, Bhatia N, Shakoori A, Ougolkov A, Liu J, et al. CRD-BP mediates stabilization of betaTrCP1 and c-myc mRNA in response to beta-catenin signalling. Nature 2006;441:898–901.
30. Yoshida K, Sanada M, Shiraishi Y, Nowak D, Nagata Y, Yamamoto R, et al. Frequent pathway mutations of splicing machinery in myelodysplasia. Nature 2011 Sep 11 [Epub ahead of print].
31. Papaemmanuil E, Cazzola M, Boultwood J, Malcovati L, Vyas P, Bowen D, et al. Somatic SF3B1 mutation in myelodysplasia with ring sideroblasts. N Engl J Med 2011 Oct 13;365:1384–95.
32. Cukier CD, Hollingworth D, Martin SR, Kelly G, Díaz-Moreno I, Ramos A. Molecular basis of FIR-mediated c-myc transcriptional control. Nat Struct Mol Biol 2010;17:1058–64.
33. Crichlow GV, Zhou H, Hsiao HH, Frederick KB, Debrosse M, Yang Y, et al. Dimerization of FIR upon FUSE DNA binding suggests a mechanism of c-myc inhibition. EMBO J 2008;27:277–89.
34. Gardina PJ, Clark TA, Shimada B, Staples MK, Yang Q, Veitch J, et al. Alternative splicing and differential gene expression in colon cancer detected by a whole genome exon array. BMC Genomics 2006;7:325–35.
35. Furumai R, Uchida K, Komi Y, Yoneyama M, Ishigami K, Watanabe H, et al. Spliceostatin A blocks angiogenesis by inhibiting global gene expression including VEGF. Cancer Sci 2010;101:2483–9.
36. Zorio DA, Bentley DL. The link between mRNA processing and transcription: communication works both ways. Exp Cell Res 2004;296:91–7.
37. Alexander R, Beggs JD. Cross-talk in transcription, splicing and chromatin: who makes the first call? Biochem Soc Trans 2010;38:1251–6.
38. Matsushita K, Tomonaga T, Kajiwara T, Shimada H, Itoga S, Hiwasa T, et al. *c-myc* suppressor FBP-interacting repressor for cancer diagnosis and therapy. Front Bios 2009;14:3401–8.
39. Hasegawa M, Miura T, Kuzuya K, Inoue A, Won KS, Horinouchi S, et al. Identification of SAP155 as the target of GEX1A (Herboxidiene), an antitumor natural product. ACS Chem Biol 2011;6:229–33.

Kobayashi et al. BMC Chemical Biology 2012, 12:2
http://www.biomedcentral.com/1472-6769/12/2

BMC
Chemical Biology

METHODOLOGY ARTICLE Open Access

Comprehensive predictions of target proteins based on protein-chemical interaction using virtual screening and experimental verifications

Hiroki Kobayashi[1†], Hiroko Harada[1†], Masaomi Nakamura[1], Yushi Futamura[1], Akihiro Ito[2], Minoru Yoshida[2], Shun-ichiro Iemura[3], Kazuo Shin-ya[3], Takayuki Doi[4], Takashi Takahashi[5], Tohru Natsume[3], Masaya Imoto[1] and Yasubumi Sakakibara[1*]

Abstract

Background: Identification of the target proteins of bioactive compounds is critical for elucidating the mode of action; however, target identification has been difficult in general, mostly due to the low sensitivity of detection using affinity chromatography followed by CBB staining and MS/MS analysis.

Results: We applied our protocol of predicting target proteins combining *in silico* screening and experimental verification for incednine, which inhibits the anti-apoptotic function of Bcl-xL by an unknown mechanism. One hundred eighty-two target protein candidates were computationally predicted to bind to incednine by the statistical prediction method, and the predictions were verified by *in vitro* binding of incednine to seven proteins, whose expression can be confirmed in our cell system.
As a result, 40% accuracy of the computational predictions was achieved successfully, and we newly found 3 incednine-binding proteins.

Conclusions: This study revealed that our proposed protocol of predicting target protein combining *in silico* screening and experimental verification is useful, and provides new insight into a strategy for identifying target proteins of small molecules.

Background

To understand complex cell systems, functional analysis of proteins has become the main focus of growing research fields of biology in the post-genome era; however, the roles of many proteins in cellular events remain to be elucidated. Among various methods to elucidate protein functions, the approach of chemical genetics is notable, with small molecular compounds used as probes to elucidate protein functions within signal pathways [1,2]. Indeed, several bioactive compounds have led to breakthroughs in understanding the functional roles of proteins [3-11]; however, one significant hurdle to developing new chemical probes of biological systems is identifying the target proteins of bioactive compounds, discovered using cell-based small-molecule screening.

A variety of methods and technologies for identifying target proteins have been reported [12]. Among them, affinity chromatography is often used for identifying biological targets of multiple small molecules of interest; however, it is usually very difficult to identify compound-targeted protein with low expression because of the low sensitivity of detection using coomassie brilliant blue (CBB) staining and MS/MS analysis. Thus, target identification of small molecules using affinity chromatography is severely limited. To overcome the limitations of affinity chromatography, we propose a new protocol combining *in silico* screening and experimental verification for identification of target proteins.

In our previous work, we developed an *in-silico* screening system, called "COPICAT" (Comprehensive Predictor of Interactions between Chemical compounds And Target proteins), to predict the comprehensive

* Correspondence: yasu@bio.keio.ac.jp
†Equal contributors
[1]Department of Biosciences and Informatics, Faculty of Science and Technology, Keio University, 3-14-1 Hiyoshi, Kohoku-ku, Yokohama 223-8522, Japan
Full list of author information is available at the end of the article

interaction between small molecules and target proteins [13]. If a target protein is input in the system, a list of chemical compounds which are likely to interact with the protein is predicted. In our previous work, several potential ligands for the androgen receptor were predicted by this system, these predictions were experimentally verified, and a novel antagonist was found [14]. On the other hand, if a chemical compound is input in the system, a list of proteins which are likely to interact with the compound is predicted by the system.

Previously, we isolated the natural product incednine from the fermentation broth of *Streptomyces* sp. ML694-90F3, which consists of a novel skeletal structure, enol-ether amide in the 24-membered macrolactam core, with two aminosugars. In addition, it was reported that incednine induced apoptosis in Bcl-xL-overexpressing human small cell lung carcinoma Ms-1 cells when combined with several anti-tumor drugs including adriamycin, camptothecin, cisplatin, inostamycin, taxol, and vinblastine [15]. Because this compound inhibits the anti-apoptotic function of Bcl-2/Bcl-xL without affecting its binding to pro-apoptotic Bcl-2 family proteins, it may target other proteins associated with the Bcl-2/Bcl-xL-regulated apoptotic pathway. To address the mode of action of incednine underlying its interesting function, we first synthesized affinity-tagged incednine which is biologically active (data not shown), and proteins bound to incednine were separated by SDS-PAGE followed by CBB staining, and each protein band was directly identified using liquid chromatography-tandem mass (LC-MS/MS) spectrometry analysis. Fifty-three proteins were identified as listed in Table 1, and some of which, such as eukaryotic initiation factor 4A3(eIF4A3), prolyl 4-hydroxylase, beta subunit (PDI), heat shock protein 70 (HSP70), and protein phosphatase 2A (PP2A) were reported to relate to cancer cell survival[16-19]. Therefore these were knocked down by siRNA or inhibited by a specific inhibitor, and assessed for their ability to modulate Bcl-2/Bcl-xL anti-apoptotic function, as does incednine. However, the candidate proteins tested did not appear to be the target responsible for modulating Bcl-2/Bcl-xL anti-apoptotic function (Additional file 1). Therefore, the target protein of incednine responsible for modulating Bcl-2/Bcl-xL anti-apoptotic function has not yet been determined, and further candidate proteins as targets of incednine are expected to emerge.

In this context, we propose a new protocol combining *in silico* screening and experimental verification for the identification of target proteins. We first predicted the candidate proteins likely binding to the input compound by applying the COPICAT system, and then employed western blotting to detect the binding of predicted proteins to the input compound. This method solves the problem of the low sensitivity of the traditional method (as illustrated in Figure 1).

Results

Computational prediction of target proteins for incednine

We set the chemical compound "incednine" as the binding ligand, and candidate proteins for the targets of incednine were computationally predicted from the KEGG database by using the statistical prediction method for protein-chemical interaction. The training dataset of protein-chemical interactions to construct the SVM-based statistical learning model was collected from the approved DrugCards data in the DrugBank database [20], and 53 interactions with incednine obtained from our previous binding experiments using affinity chromatography (see Table 1 and Methods) because the prediction accuracy was increased when more training samples of protein-chemical interactions were given to the SVM-based statistical learning model. Among 24,245 human proteins in the KEGG repository, 182 proteins were newly predicted as positive, that is, to interact with incednine with high probability greater than the 0.5 threshold (the default threshold value).

Clustering of computationally predicted proteins

The 182 proteins that were computationally predicted to bind to incednine were clustered by the hierarchical clustering method using 199-dimentional feature vector that was used for encoding amino acid sequences to construct the SVM-based statistical learning model (See Methods section for the details). Note that the similarity based on this 199-dimentional feature vector is different from the sequence similarity, and this similarity measure based on the 199-dimentional vector was proven to work well for protein-chemical interaction predictions in our previous work [13]. For example, 5HTT and AR α-1A showed only about 10% sequence similarity although both were reported to interact with the MDMA drug and successfully predicted by our SVM-based statistical learning method. A cutoff threshold on the constructed clustering tree was determined so that the proteins were clustered into 11 clusters and each cluster had a statistically significant number of members. The proteins predicted to bind to incednine are listed in Additional file 2.

Experimental verification

Next, to examine whether incednine can bind to the proteins, an *in vitro* biotinylated incednine pull-down assay using the lysate of Bcl-xL expressing Ms-1 cells was performed. We tested 16 proteins as pilot experiments, which are selected from each cluster by one or two based on antibody availability. Negative candidates that were predicted not to bind to incednine were extracted for experimental verification. These proteins, positive candidates and negative candidates, are listed in Table 2. Among positive candidate proteins, 2 positive candidates PIK3CG and ACACA were found to bind to

Table 1 List of proteins identified to bind to incednine in our previous binding experiments

Protein	Uniprot ID	Kegg ID
poly 4- hydroxylase, beta submit	P07237	5034
N-acylaminoacyl peptide hydrolase	P13798	327
Heat shock protein 70	P08107	3303/3304
Protein Phosphatase A2	P67775	5515
Similar to DNA damage-binding protein 1	Q16531	1642
Deoxyhypusin synthase isoform alpha	P49366	1725
Methionine adenosyltransferse alpha/beta	P31153/Q00266/Q9NZL9	4144/4143/27430
4-alpha-glucanotransferse	P35573	178
Actin alpha 4	O43707	81
Eukaryotic Initiation factor 4A3	P38919	9775
Deoxycytidine kinase	P27707	1633
ATP synthase H+ transporting, mitochondrial F1complex, alpha	P25705	498
prohibitin	P35232	5245
proteasome alpha 7subuit	O14818	5688
proteasome(prosome,macropain) subunit alpha type 8	Q8TAA3	143471
centaurin,beta 2	Q15057	23527
heterogeneous nuclear ribonucleoprotein A/B	Q99729	3182
heterogeneous nuclear ribonucleoprotein K	P61978	3190
heterogeneous nuclear ribonucleoprotein D	Q14103	3184
heterogeneous nuclear ribonucleoprotein A2/B1	P22626	3181
heterogeneous nuclear ribonucleoprotein A1	P09651	3178
heterogeneous nuclear ribonucleoprotein M	P52272	4670
small nuclear ribonucleoprotein polypeptide D2 family	P62316	6633
mitochondrial riblosomal protein L2	Q5T653	51069
mitochondrial riblosomal protein L20	Q9BYC9	55052
mitochondrial riblosomal protein L3	Q6IBT2	11222
mitochondrial riblosomal protein L40	Q9NQ50	64976
mitochondrial riblosomal protein L46	B2RD75	26589
mitochondrial riblosomal protein L49	B2R4G6	740
mitochondrial riblosomal protein L1	A6NG03	65008
mitochondrial riblosomal protein L37	Q9BZE1	51253
small nuclear ribonucleoprotein-assosiated protein B and B'	P14678	6628
cAMP-dependent protein kinase, regulatory subunit alpha 1	P10644	5573
phosphoribosyl pyrophosphate synthetase-associated protein 1	B2R6M4	5635
peptidylprolyl isomerase-like 2	Q13356	23759
thymoprotein isoform beta, gamma	P42167	7112
fructose-bisphosphate aldolase A	P04075	226
brain creatine kinase	P12277	1152
enolase 1	P06733	2023
Ewing sarcoma breakpoint region 1	Q5THL0	2130
fusion(involved in t(12;16) in malignant liposarcoma)	Q6IBQ5	2521
GDP dissociation inhibitor 2	Q5SX88	2665
nucleosome assembly protein 1-like 1	P55209	4673
nucleosome assembly protein 1-like 4	Q99733	4676

Table 1 List of proteins identified to bind to incednine in our previous binding experiments *(Continued)*

phosphoglycerate dehydrogenase	O43175	26227
triosephosphate isomerase 1	P60174	7167
clathrin heavy chain 1	Q00610	1213
clathrin heavy poly peptide -like 1	P53675	8218
glutamyl-prolyl tRNA synthetase	P07814	2058
retinoblastoma binding protein 7	Q16576	5931
retinoblastoma binding protein 4	Q09028	5928
tripartite motif-containing 28 protein	Q13263	10155
high glucose-regulated protein 8	Q9Y5A9	51441

incednine, and 5 positive candidates DAPK1, PIK3C2B, PIP5K3, CHD4, GTF2IRD2 did not bind to incednine. Among negative candidate proteins, 2 negative candidates BECN1 and KIF5B did not bind to incednine, and 1 negative candidate PARP1 did bind to incednine (Figure 2). On the other hand, ITPR1, PARP14, PLCB1, KIF1A, KIF21B, and RGPD5, listed as positive candidates in Table 2, were not well expressed and were not detected in Bcl-xL-expressing Ms-1 cells; therefore, accuracy of 40% (4/10), sensitivity of 66.7% (2/3) and precision of 28.6% (2/7) were achieved.

Discussion

For target identification using affinity chromatography, conventional method requires multiple steps as follows; SDS-PAGE, CBB staining, excision of gel, destaining, reduction, trypsinization, and application to LC-MS/MS system (7 steps); these steps can be cumbersome, time-consuming and require expensive installation. Furthermore, CBB staining used in conventional method can detect proteins over nanogram order. In contrast, our proposed protocol for predicting target protein allows us to use western blotting to detect proteins in picogram order. Indeed, we found two incednine-binding proteins by this prediction. Additionally, we can enhance the precision of COPICAT by feeding back the experimental results to the system.

In this work, PIK3CG, PARP1, and ACACA were revealed to bind to incednine by applying our protocol to identify potential target proteins of chemical compounds. These proteins are potential targets of incednine because it has been reported that these proteins are related to cancer survival and drug resistance, as follows.

PI3KCG encodes p110 catalytic subunit isoform p110γ and heterodimerizes with regulatory subunit p101, composing class IB PI3K in the PI3K family [21,22]. Although PIK3CG and PIK3C2B are distant homologous

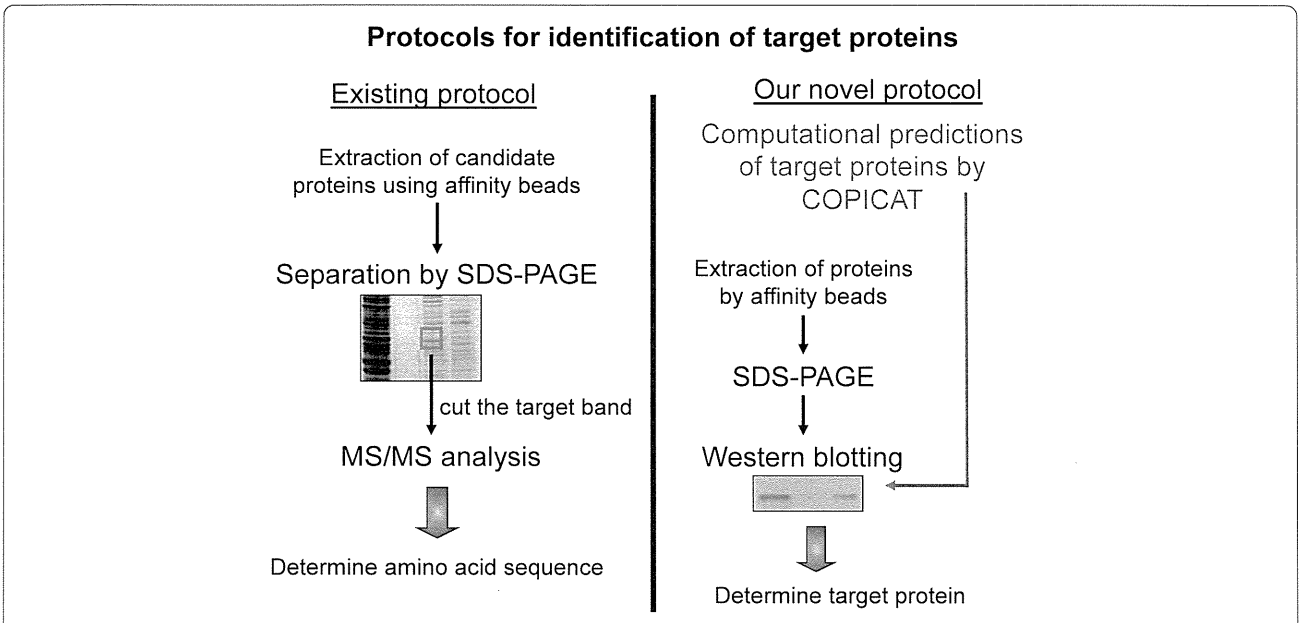

Figure 1 Schematic illustration of our protocol combining *in silico* screening and experimental verification for identification of target protein.

Table 2 Representative proteins selected from each cluster and negative candidates for experimental verification

Cluster No.	Representative Protein
1	ITPR1 (inositol 1,4,5-triphosphate receptor, type 1)
2	DAPK1 (death-associated protein kinase 1)
3	PIK3CG (phosphoinositide-3-kinase, catalytic, gamma polypeptide), PIK3C2B (phosphoinositide-3-kinase, class 2, beta polypeptide)
4	PARP14 (poly (ADP-ribose) polymerase family, member 14)
5	PIP5K3 (phosphatidylinositol-3-phosphate/phosphatidylinositol 5-kinase, type III)
6	PLCB1 (phospholipase C, beta 1)
7	CHD4 (chromodomain helicase DNA binding protein 4)
8	KIF1A (kinesin family member 1A), KIF21B (kinesin family member 21B)
9	ACACA (acetyl-Coenzyme A carboxylase alpha)
10	GTF2IRD2 (GTF2I repeat domain containing 2)
11	RGPD5 (RANBP2-like and GRIP domain-containing protein 5)
Negative	Proteins predicted not to bind to incednine
1	BECN1 (Beclin-1)
2	PARP1 (poly (ADP-ribose) polymerase family, member 1)
3	KIF5B (kinesin family member 5B)

with 20% sequence identity, incednine selectively binds to PIK3CG but not PIK3C2B (Figure 2). In contrast to class IA, class IB PI3K acts downstream of G-protein coupled receptors (GPCR). It has been reported that p110γ was upregulated and activated by the chimeric oncogene Bcr-Abl expression to contribute to cell proliferation and drug resistance in chronic myelogenous leukemia [23], and was found to be highly and specifically expressed among the PI3K family in human pancreatic cancer [24], suggesting that class IB PI3K might relate to cell survival and drug resistance. Product of enzymatic activation of class IB PI3K as class IA, phosphatidylinositol-3,4,5-trisphosphate, makes BAD dissociate from Bcl-xL and promotes cell survival *via* Akt activation [22]. Therefore class IB PI3K might contribute cell survival in Bcl-xL-overexpressing cells.

PARP1 is a member of the PARP protein superfamily that catalyzes the polymerization of ADP-ribose moieties onto target proteins, using NAD^+ as a substrate and releasing nicotine amide in the process [25]. PARP1 activity is important for the regulation of homeostasis and the maintenance of genomic stability, participating in DNA repair, the regulation of transcription, DNA replication, cell differentiation, proliferation and cell death [26-28]. Many *in vitro* and *in vivo* experiments demonstrated that inhibition of PARP1 potentiates the cytotoxicity of anti-cancer drugs and ionizing radiation [29-32]. Therefore, incednine could bind to PARP1 and could function as antagonist of anti-apoptotic PARP1 protein. Alternatively, PARP1 is emerging as an important activator of caspase-independent cell death. It has been previously reported that PARP1 mediates the release of apoptosis-inducing factor (AIF), one of the initiators of

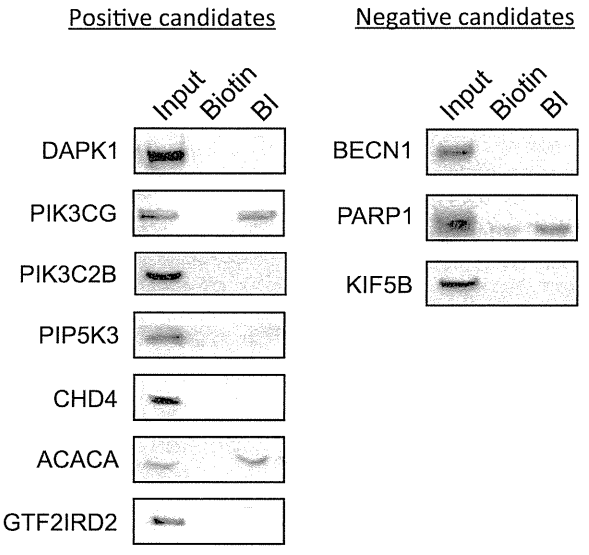

Figure 2 Experimental verification by *in vitro* biotinylated incednine pull-down assay. Lysates from Ms-1 overexpressing Bcl-xL were incubated with biotin (Biotin) or biotinylated incednine (BI) and avidin beads for 3 h. The beads were washed, and co-precipitated proteins were eluted with 2 mM biotin. The eluted proteins were subjected to western blotting using the indicated antibodies. "Positive candidates" means proteins which were predicted to bind to incednine, and "Negative candidates" means proteins which were predicted not to bind to incednine.

caspase-independent cell death, possibly due to enzymatic over-activation [33-35]. We also observed that co-treatment of Bcl-xL-overexpressing Ms-1 cells with incednine and ant-tumor drugs induced AIF release and subsequent caspase-independent cell death (unpublished data); therefore, we can not exclude the possibility that incednine binds to PARP1 and functions as PARP1 agonist by accerelating AIF release.

However, the most likely candidate of an incednine target protein is ACACA (acetyl-CoA carboxylase-α), which was classified in cluster 9. ACACA is the rate-limiting enzyme for long-chain fatty acid synthesis that catalyzes the ATP-dependent carboxylation of acetyl-CoA to malonyl-CoA, playing a critical role in cellular energy storage and lipid synthesis [36]. There is strong evidence that cancer cell proliferation and survival are dependent on *de novo* fatty acid synthesis [37-40]. Additionally, ACACA is upregulated in multiple types of human cancers [41,42]; therefore, ACACA may also contribute to cell survival in Bcl-xL-overexpressing tumor cells. Indeed, our preliminary experiments suggested that chemical inhibition of ACACA using TOFA (5-tetradecyloxy-2-furoic acid, ACACA antagonist) or small interfering RNA-mediated ACACA silencing results in the induction of apoptosis in Bcl-xL-overexpressing human small cell lung carcinoma Ms-1 cells when combined with anti-tumor drugs as does incednine (unpublished observation), suggesting that ACACA might be a molecular target of incednine. The possibility that incednine targets ACACA is being actively investigated.

While our experimental verification implied the relatively low precision value 28.6% (2/7), new detections of two incednine-binding proteins in addition to previously identified 53 proteins are significant. On the other hand, while we selected 7 candidates by clustering 182 predicted proteins for experimental verification, more comprehensive verification experiments for the 182 predicted proteins are needed.

The application of our method to incednine resulted in 28.6% (2/7) precision according to *in vitro* pull-down assay. However, this relatively low precision value does not represent the true statistical significance of the method and is not comparable to the benchmark performances (including 98.4% precision) by 10-fold cross-validation for COPICAT system.

This 28.6% precision can be evaluated by using the following *P*-value.

$$P\text{-}value = \sum_{x=p}^{t} \frac{{}_{M}C_{x} \times {}_{(N-M)}C_{(t-x)}}{{}_{N}C_{t}}$$

Here, N is the number of human proteins, M is the number of proteins potentially binding to the incednine, t is the number of tested proteins, and p is the number of true positives. With N =24,245, which is the number of human proteins in the KEGG repository, and $M = N \times 1\% \fallingdotseq 243$, which is based on the overestimated assumption that 1% of all proteins could be regarded as potential binding proteins for the incednine. This *P*-value defines the probability that the prediction precision can be obtained by random selection of proteins. Then, *P*-value of 0.002 was obtained for the prediction precision 28.6%. This small *P*-value means that 28.6% (2/7) precision can be obtained with very small chance by random selection, and therefore, this small *P*-value proves the validity of our method.

Conclusions

Although further study is required for complete determination of the target protein of incednine, this study demonstrated that our proposed protocol of predicting target protein combining *in silico* screening and experimental verification is useful, and provides new insight into a strategy for identifying target proteins of small molecules.

Methods

Training datasets

The DrugBank dataset was constructed from Approved DrugCards data, which were downloaded from the DrugBank database [20]. These data consist of 964 approved drugs and their 456 associated target proteins, constituting 1,731 interacting pairs or positives. Additional data about 53 interactions with incednine, listed in Table 1, were obtained from our previous binding experiments.

Feature vectors

An amino acid sequence of protein is divided into trimers (three amino acid residues), and all of the 8,000 trimers are clustered into 199 groups according to physical-chemical properties. Then, an amino acid sequence is converted to a 199-dimensional feature vector based on the frequencies of 199 clusters (See for [13] the details of this procedure). A chemical compound is also converted to another feature vector of 199 dimension representing substructure statistics extracted from the structural formula of a chemical compound. The size of the dimensions, that is, 199 dimensions, was determined based on the variance of each dimension. The top 199 dimensions with significantly diverse variances in statistical classification were selected.

Statistical prediction method for protein-chemical interaction

We developed a comprehensively applicable statistical prediction method for interactions between any proteins